Performance of Cooperative Space Time Coding with Spatially Correlated Fading and Imperfect Channel Estimation

by

DERRICK CHE-YU WAN

B.A.Sc., The University of British Columbia, 2005

A THESIS SUBMITTED IN PARTIAL FULFILLMENT OF

THE REQUIREMENTS FOR THE DEGREE OF

MASTER OF APPLIED SCIENCE

in

THE FACULTY OF GRADUATE STUDIES

(Electrical and Computer Engineering)

THE UNIVERSITY OF BRITISH COLUMBIA

(Vancouver)

February 2008

Abstract

A performance evaluation of CSTC (Cooperative Space Time Coding) with spatially correlated fading and imperfect channel estimation in Gaussian as well as impulsive noise is presented. Closed form expressions for the pairwise error probability conditioned on the estimated channel gains are derived by assuming the components of the received vector are independent given the estimated channel gains. An expurgated union bound using the limiting before averaging technique given the estimated channel gains is then obtained. Although this assumption is not strictly valid, simulation results show that the bound is accurate in estimating the diversity order as long the channel estimation is not very poor. It is found that CSTC with block fading channels can reduce the frame error rate (FER) relative to SUSTC (Single User Space Time Coding) with quasi-static fading channels, even when the channel gains for each user are strongly correlated and when the channel estimations are very poor.

A decision metric for CSTC with spatially correlated fading, imperfect channel estimation, and impulsive mixture Gaussian noise is derived which yields lower FERs than the Gaussian noise decision metric. Simulation results show that the FER performance of CSTC with mixture Gaussian noise outperforms CSTC with Gaussian noise at low SNR. At high SNR, the FER performance of CSTC with Gaussian noise is better than the FER performance of CSTC with mixture Gaussian noise due to the heavy tail of the mixture Gaussian noise.

Contents

List of Tables

List of Figures

List of Abbreviations and Symbols

Acronyms

AWGN	Additive white Gaussian noise
AF	Amplify and Forward
BER	Bit Error Rate
BPSK	Binary Phase Shift Keying
CDMA	Code Division Multiple Access
CRC	Cyclic Redundancy Check
CSI	Channel State Information
CSTC	Cooperative Space Time Coding
DF	Detect and Forward
FER	Frame Error Rate
GDM	Gaussian Decision Metric
MGDM	Mixture Gaussian Decision Metric
MRRC	Maximum Ratio Receiving Combining
MLE	Maximum Likelihood Estimation
PEP	Pairwise Error Probability
r.v.	Random Variable
RF	Radio Frequency
RCPC	Rate Compatible Punctured Convolutional Codes
SNR	Signal to Noise Ratio
ST	Space Time
STTC	Space Time Trellis Code

STBC	Space Time Block Code
STD	Simple Transmit Diversity
SUSTC	Single User Space Time Coding
UB	Upper Bound
VA	Viterbi Algorithm
3G	3^{rd} Generation

Operators and Notation

$\lvert\cdot\rvert$	Absolute value of a complex number
$\mathcal{E}\{\cdot\}$	Expectation
$\det(\cdot)$	Determinant
$[\cdot]^*$	Complex conjugate
$[\cdot]^T$	Matrix or vector transposition
$[\cdot]^H$	Matrix or vector hermitian transposition
$\Re\{\cdot\}$	Real part of a complex number
$\Im\{\cdot\}$	Imaginary part of a complex number

Acknowledgments

I would like to extend my sincere thanks to my supervisor, Dr. Cyril Leung, who has given me the chance to pursue my interest in wireless communication, and has always been there to provide me with invaluable guidance, and insights into my research. He has taught me the importance of fundamental knowledge in the field and how to solve a problem most efficiently, which will be a very important asset for pursuing my career.

I would also like to thank Dr. Paul Lusina who has given me useful suggestions on my research.

Finally, I would like to thank my mother and my sister who have always encouraged me to stay motivated and been supportive of my quest to pursue higher education. I would not have been able to complete this thesis without them.

This work was partially supported by the Natural Sciences and Engineering Research Council Grant OGP0001731.

Chapter 1

Introduction

Two important goals for third generation (3G) cellular communication systems are to achieve high voice quality and provide high bit rate data services. However, due to the nature of the wireless propagation environment, time-varying multi-path fading causes the received signal strength to vary significantly, thereby making it difficult to achieve reliable communication [1]. The concept of diversity, which is to provide the receiver with multiple versions of the information bearing signals that are subjected to fading, has been shown to be very effective in mitigating the effects of multi-path fading. Some well known forms of diversity are space, time, frequency, and polarization diversity [2]. Time and frequency diversity use different time slots and frequency bands to transmit signals. Multiple antennas with different polarizations for reception and transmission are used in polarization diversity. Space diversity uses different propagation paths. Antennas are spatially separated so that the paths from transmit antennas to receive antennas undergo more or less independently fading.

Space diversity, also known as antenna diversity, can be divided into two groups: receive and transmit diversity. Receive diversity makes use of multiple receive antennas that are well separated to ensure independent fading. Some known forms of receive diversity include selection, switched, equal gain, and maximal ratio combining diversity [2]. Similarly, transmit diversity uses multiple transmit antennas which are spatially separated. Previous work on transmit diversity can be broadly divided into two categories: systems with feedback and systems without feedback. Generally, a system with feedback has a better performance. For example, with channel state information (CSI) at the transmitter, optimal transmit weights can be calculated to maximize the desired received signal power at the receiver and minimize the interference with other nearby receivers [3]. However, extra signalling overhead is required for systems with feedback.

A system without feedback generally has a poorer performance. The signalling overhead for such a system is lower and the the receiver is simpler [3]. Space-time (ST) coding over multiple transmit antennas is often used when CSI is unknown and can be divided into two forms: ST trellis coding (STTC) and ST block coding (STBC) [4]. For STTC, the space time encoder chooses the constellation points for each input symbol to simultaneously transmit from each antenna so that the coding and diversity gains are maximized. STTC often requires higher decoding complexity due to the complexity of the trellis structure. Maximum likelihood estimation (MLE) is often implemented using a viterbi algorithm (VA) where the trellis path with the smallest accumulated distance is chosen [4]. An example of STBC is the Alamouti coding [5] which is attractive for its particularly simple decoding scheme.

1.1 Motivation and Goals

Many wireless systems, such as cellular, ad-hoc, and sensor networks, have size, power and complexity constraints which limit the use of conventional transmit diversity methods [2]. For example, in the uplink of cellular systems, the size of the mobile station is a constraint. More recently, a "cooperative diversity" technique in [6, 7] has been proposed which can achieve the same diversity order as conventional transmit diversity schemes, while alleviating the size, power, and complexity problems associated with conventional transmit diversity schemes.

The idea in cooperative diversity is that each node in the network is assigned "partners" whenever possible. Each of the partners in the network transmits not only its own information but also the information for its partners as well. Thus, it establishes a virtual antenna array and enables the nodes to achieve higher data rates and diversity orders than what they could achieve on their own. Figure 1.1 shows an example

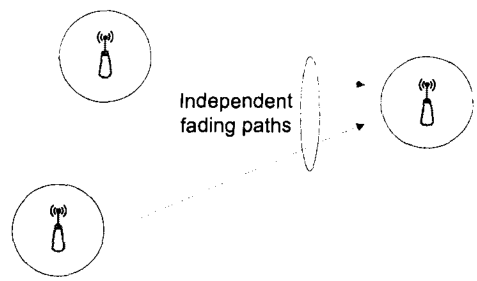

Figure 1.1: Cooperative Diversity

where there are two mobile users, each with one antenna communicating with the destination. Diversity cannot be achieved by each user individually since there is only one transmit antenna at each user. However, by broadcasting its information to the other user and having the other user forward some version of the received information, along with its own data to the destination, transmit diversity can be achieved.

The earlier proposed methods used for user cooperation often have the users *repeat* the information received from the other users [8, 9]. These repetition methods can be generally divided into two forms: Amplify-and-Forward (AF) and Detect-and-Forward (DF). In AF, the users simply amplify and retransmit their received signals whereas in DF the users fully decode, re-encode, and re-transmit each other's information. Recent research work involves a combination of cooperative diversity with channel coding and space time coding. Instead of repeating the received information, the users attempt to decode the partners' information and transmit added parity symbols according to some chosen coding scheme.

Most of the studies use idealized assumptions such as independent fading and perfect channel estimation [6, 7, 8, 9]. In practice, insufficient antenna spacing can cause the channel gains to be dependent and noise can cause the channel estimation to be imperfect at the receiver. Numerous studies have examined the bit error rate (BER) performance of conventional transmit diversity schemes in different channel conditions. For example, in [10, 11], the performance degradations of the simple transmit diversity (STD) technique with time-selective, spatially correlated fading, and imperfect channel estimation error were studied. Performance analyses of the space time codes with imperfect channel estimation error are provided in [12, 13]. In this thesis we analyze the performance degradation of one particular cooperative space time coding scheme due to spatially correlated fading and imperfect channel estimation.

1.2 Outline of Thesis

In Chapter 2, a review of related work on cooperative diversity is presented. In Chapter 3, performance bounds on the proposed CSTC system with spatially correlated fading and imperfect channel estimation are derived. In Chapter 4, these bounds are compared to simulation results. In Chapter 5, the effect of impulsive noise is studied and the gain obtained using a decision metric for non-Gaussian noise is examined. A summary of the main contributions and findings as well as some recommendations for future work are provided in Chapter 5.

Chapter 2

Background and Related Work

In this chapter, we present a summary of related published work on cooperative communication. In particular, the cooperative space time coding protocol model in [14] is reviewed as it is adopted in the thesis.

2.1 Relay Channel

The basis of cooperative communication comes from the idea of the relay channel that was proposed in [15] and shown in Figure 2.1.

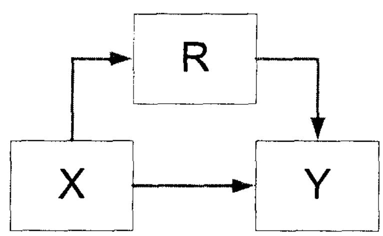

Figure 2.1: Relay Channel.

There is one sender, X, and one receiver, Y, with an intermediate node, R, which acts as a relay to help the communication from X to Y. First, X transmits its information to R and Y, then R transmits X's information to Y to help Y decode X's information more successfully. This model can be viewed as consisting of two parts: a broadcast channel (X to R and Y) and a multiple access channel (R and X to Y). The work in [15] evaluated certain non-faded relay channels, derived its lower and upper bounds on capacity, and concluded that the overall capacity is better than individual capacities achievable without relay in many cases. However, in [15] it was assumed that the relay can transmit and receive at the same time, which is not often practical. Later, the model was extended to multi-path fading [6, 8, 16], and additional constraints were added so that the source and relay transmit on orthogonal (in time or frequency) channels.

2.2 Block Fading Channel

The block fading model is a useful approximation for a time varying fading channel when fading is not fast enough to be represented as a temporally i.i.d process, but it is also not slow enough to be well approximated by a quasi static model [17]. Information bits are coded/modulated into F blocks of length N symbols, resulting a codeword of length NF symbols. The NF symbol codeword is referred to as a frame and shown as

$$\mathbf{C} = \begin{bmatrix} C_{1,1} & C_{1,2} & C_{1,3} & \dots & C_{1,N} \\ C_{2,1} & C_{2,2} & C_{2,3} & \dots & C_{2,N} \\ . & . & \dots & . & . \\ . & . & \dots & . & . \\ C_{F,1} & C_{F,2} & C_{F,3} & \dots & C_{F,N} \end{bmatrix}. \tag{2.1}$$

For a block fading channel, each of the F blocks is assumed to undergo different fading but the channel is time-invariant during each block. For example, the model used in this thesis has a frame of two blocks when cooperation takes place with each block consisting of a codeword of length 130 symbols as follows

$$\mathbf{C} = \begin{bmatrix} C_{1,1} & C_{1,2} & C_{1,3} & \dots & C_{1,130} \\ C_{2,1} & C_{2,2} & C_{2,3} & \dots & C_{2,130} \end{bmatrix}. \tag{2.2}$$

2.3 Impulsive Noise

Impulsive noise has been used in characterizing man-made RF noise and low frequency atmospheric noise [18]. For such situations, the commonly used Gaussian Noise model is often not appropriate. Unlike Gaussian noise, the probability density function (pdf) of impulsive noise has a heavier tail, causing a large deviation from the mean. Some commonly used impulsive noise models, such as generalized Gaussian and Cauchy noise, Mixture Noise, Middleton Class A noise, and Laplace noise have been discussed in [18]. One common feature that all of these non-Gaussian noise models share is that the tails of their noise density function decays at rates lower than the rate of delay of the Gaussian Noise model. In [19, 20], the performance bounds of systems with Class-A Middleton noise is analyzed. It is shown that the real part and the imaginary part of the complex Mixture Gaussian noise are statistically dependent. In this thesis, we focus on Gaussian Mixture Noise.

Mixture noise is one kind of widely used impulsive noise model. Its pdf is

$$p_N(n) = (1-\epsilon)\eta(n) + \epsilon I(n) \tag{2.3}$$

where ϵ is the impulsive index, a constant value, $\eta(n)$ is a Gaussian representing the background noise, I(n) is some other density function with a heavier tail that represents the impulsive noise. When I(n) is also a Gaussian, $p_N(n)$ is a mixture Gaussian noise and the pdf is given by

$$P_N(n) = (1-\epsilon)\frac{1}{\sqrt{2\pi\sigma_\eta^2}}\exp\left[-\frac{n^2}{2\sigma_\eta^2}\right] + \epsilon\frac{1}{\sqrt{2\pi\sigma_I^2}}\exp\left[-\frac{n^2}{2\sigma_I^2}\right] \tag{2.4}$$

where σ_η^2 is the variance of the background noise and σ_I^2 is the variance of the impulsive noise. The total noise variance is $(1-\epsilon)\sigma_\eta^2 + \epsilon\sigma_I^2$. The ratio $\frac{\sigma_I^2}{\sigma_\eta^2}$ and the impulsive index ϵ are usually in the range [20,10000] and [0.01, 0.33] respectively [18].

Figure 2.2 compares the Gaussian Noise with Mixture Gaussian Noise. Different $\frac{\sigma_I^2}{\sigma_\eta^2}$ and ϵ values of the Mixture Gaussian Noise are provided. It is observed that a smaller ϵ and

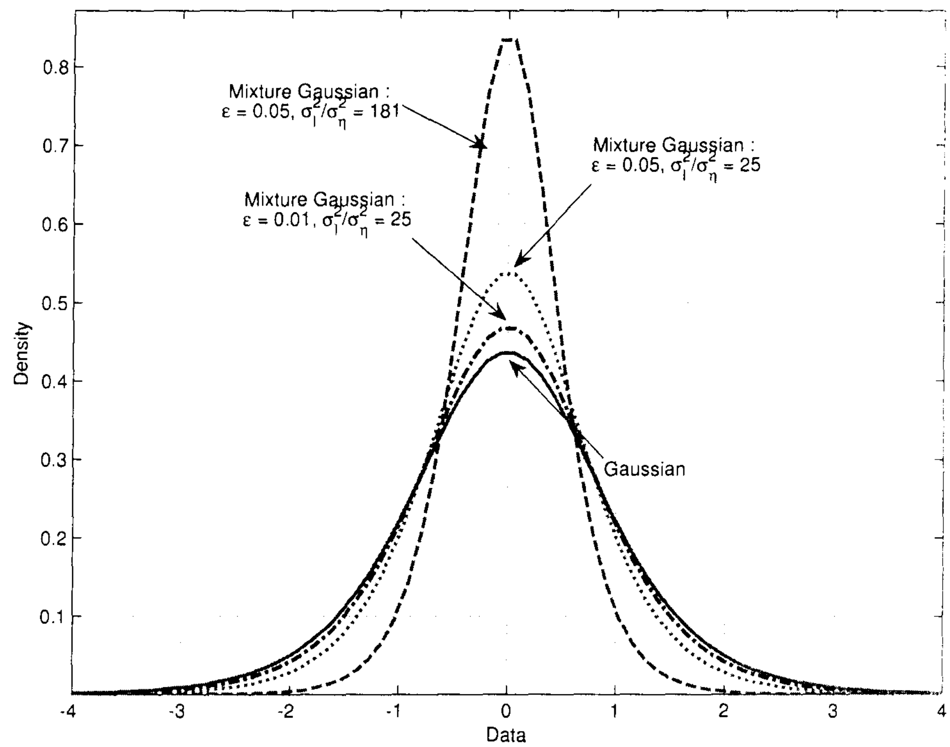

Figure 2.2: Comparison of Gaussian and Mixture Gaussian pdf's. All pdf's have a variance of 1

$\frac{\sigma_I^2}{\sigma_\eta^2}$ imply a heavier tail in the pdf. All pdf's have a variance of 1.

2.4 Cooperative Communication

Cooperative communication is similar to the relay channel in that they both use the concept of relaying information from another node to achieve diversity. In the relay channel, the relay only helps the user to transmit information on a different path and does not carry its own information. However, in the cooperative communication model, each user not only transmits its own information; it also acts as a relay to its chosen "partner". As a result, the same diversity order as conventional transmit diversity schemes, such as Alamouti and maximum ratio receive combining (MRRC) [14, 5] can be achieved. A general concept of "User Cooperation" was first presented in [6, 7] and a general information-theoretic model for two users was used to analyze the achievable rate region and outage probability. A CDMA-based implementation of the DF scheme was then proposed. It was observed in [6, 7] that under most scenarios, user cooperation allows an increase in system throughput and cell coverage, and a decreased sensitivity to channel variations. In general, cooperative communication methods can be divided into two general groups: amplify and forward and detect and forward.

2.4.1 Amplify and Forward (AF)

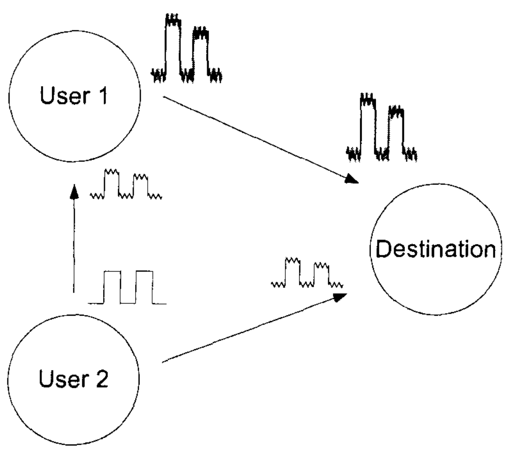

Figure 2.3: Amplify and Forward.

The AF method is shown in Figure 2.3. Each user first receives a noisy version of its partner's information. The users simply amplify and retransmit the noisy signal to the receiver. It is shown in [8] that although a noisy version of the partner's information is amplified, the receiver is still able to receive two independent versions of the desired information, thus allowing the receiver to better decode the information. The AF method was proposed in [21] and the BER performance was analyzed. It was shown that despite the noise propagation from the partner, AF outperforms non-cooperative transmission. Later in [9], the outage probability for AF in quasi-static Rayleigh fading was analyzed. It was found that AF signalling achieves a diversity order of two for two users.

2.4.2 Detect and Forward (DF)

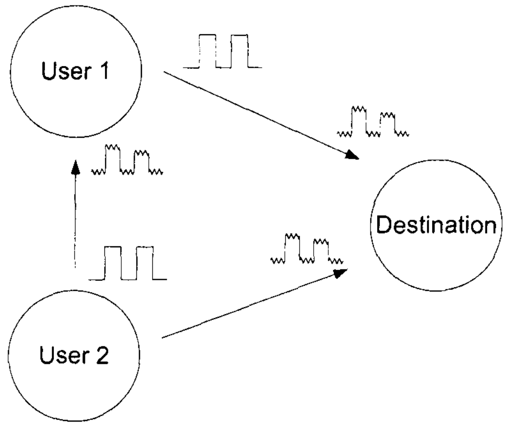

Figure 2.4: Detect and Forward.

The DF method is shown in Figure 2.4. As in the AF method, each user receives a noisy version of its partner's information. Instead of amplifying the noisy signal, the partner attempts to decode the information and retransmit an estimate of its partner's information to the receiver. In [8], it is shown that error propagation may arise if the partner decodes incorrectly and retransmits the erroneous information to the receiver. A hybrid DF method was proposed in which the partner only transmits the user's information when the signal to noise ratio (SNR) between the user and its partner is high. When the SNR between the user and its partner is low, the user reverts back to the non-cooperative transmission.

The AF and DF methods discussed in [9] involve a user repeating the modulated symbols transmitted by its partner. From a channel coding point of view, this approach is not the most efficient. A new cooperative framework termed "coded cooperation" was introduced in [16] in which cooperative signaling is combined with channel coding.

By having the users transmit on orthogonal channels enables the destination to separately detect each user. Figure 2.5 shows an implementation for a TDMA system used in [22].

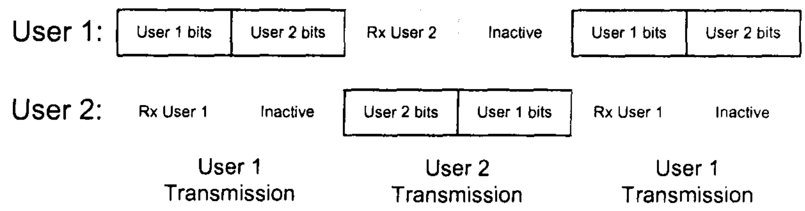

Figure 2.5: TDMA Implementation for Coded Cooperation.

In [22], each user has a N-bit codeword to be transmitted. The two users cooperate by dividing their N-bit codewords into two time segments. In the first segment, each user transmits a codeword with N_1 bits and attempts to decode its partner's transmission. If the user successfully decodes the partner's code word (through error detection such as CRC code), the user transmits N_2 additional parity bits for its partner according to some overall coding scheme in the second segment where $N_1 + N_2 = N$. Otherwise, the user transmits the parity symbols for its own information. The users do not have knowledge of whether their own first segments were correctly decoded. Hence, the destination must know the decision made in the second segment by each user. One approach is for each user to send one additional bit in the second segment to indicate the decision made in the first segment. The other approach is for the destination to decode all possible scenarios, thus increasing the complexity at the destination. It was indicated in [22] that the proposed model is flexible in that it can be implemented with either block or convolutional codes. Rate-compatible punctured convolutional code (RCPC) was implemented in [22] and the BER and FER performances were studied for both slow and fast fading. It was found that coded cooperation can achieve significant gains compared to a non-cooperative system while maintaining the same information rate, transmitting power, and bandwidth.

In [23], "space time cooperation" was introduced which combined space time coding with "coded cooperation." The main difference between space time cooperation and coded cooperation is that the users send both their own and their partner's parity bits in the second segment. However, some implementation issues such as the transmission in both channels in the second segments and coherent combining at the receiver were discussed. It was found that space time cooperation provides better performance than coded cooperation in fast fading when the two user uplink channels have unequal average SNR. The user with the better channel has to sacrifice its performance to help the user with the worse channel in "coded cooperation" whereas in "space time cooperation", the performance for both users improves [23].

2.5 Cooperative Space Time Coding (CSTC)

The Cooperative Space Time Coding protocol proposed in [24, 14] is used throughout the thesis. Performance analysis of two users with multiple transmit and receive antennas was discussed in [14]. In this thesis, we consider two users, U_1 and U_2, each with two transmit antennas and one destination node with one receive antenna.

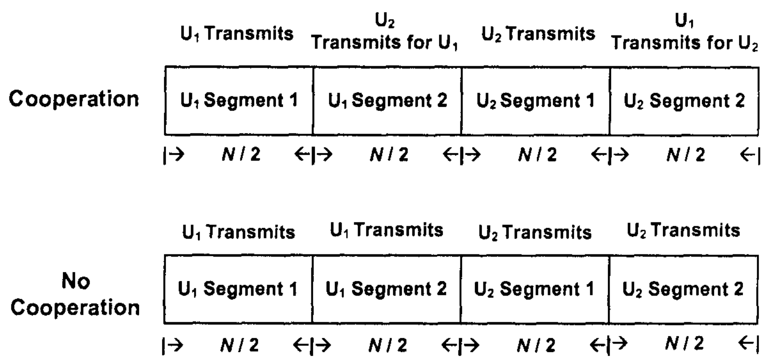

Figure 2.6: Time Division Channel Allocations.

The cooperative model in [8, 22, 24, 14] uses time division channel allocations among the users as shown in Figure 2.6 for cooperation and no cooperation. In either case, there is a total of N time slots, which will term a frame, assigned to each user. The N time slots are divided into two halves: segment 1 and segment 2. This leads to $N/2$ slots for U_1 to broadcast its coded bits in the first segment and $N/2$ slots for possible cooperation in the second segment. Since the FER analysis for U_1 is symmetric to the FER analysis of U_2, we only analyze the performance of U_1 for simplicity.

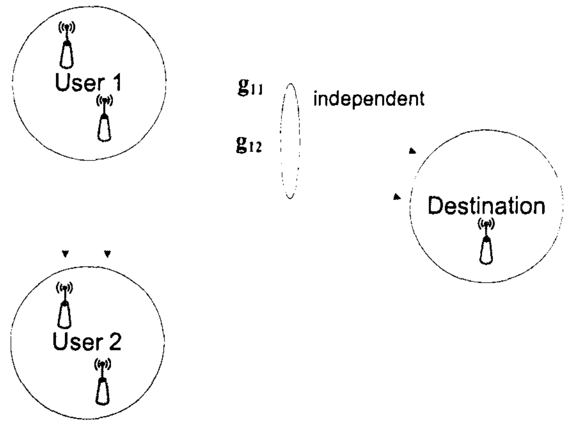

Figure 2.7: Transmission Scheme : Segment 1.

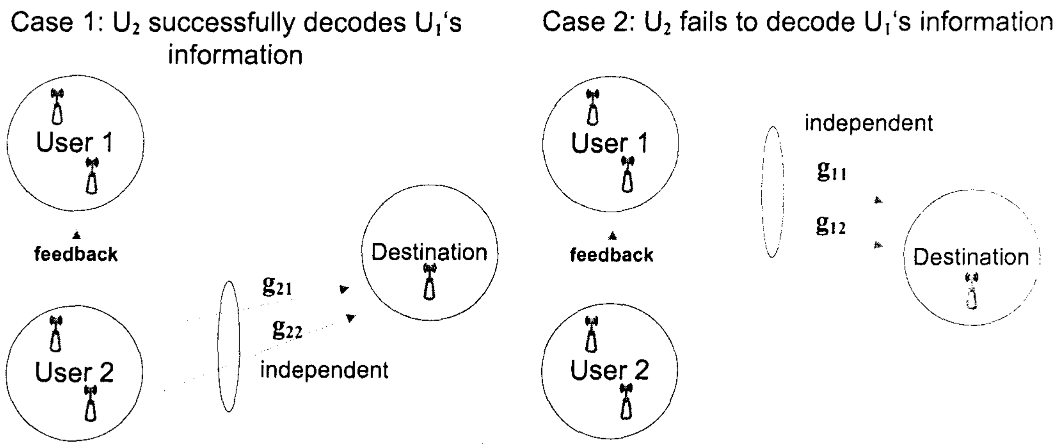

Figure 2.8: Transmission Scheme : Segment 2.

Figures 2.7 and 2.8 explain the transmission in the two segments. The channel gains of antenna i (i = 1,2) for U_1 and U_2 are denoted by $g_{1,i}$ and $g_{2,i}$ and are assumed to be outcomes of independent zero-mean complex Gaussian r.v's with variance 0.5 per dimension and are constant during the two segments for a given user. The path gains for the two users as well as those for different antennas of the same user are assumed to be independent as indicated in Figure 2.7 and 2.8. The first segment is used for U_1 to broadcast its coded bits to the receiver and U_2. In the second segment, U_2 informed U_1 if the coded bits have been successfully received. If U_2 successfully decodes U_1's information, U_2 transmits the remaining coded bits for U_1 in the second segment. If U_2 fails to decode

U_1's information, U_1 continues to transmit the remaining coded bits in the second time segment. This makes the scheme easier to be applied in most applications since the new scheme is exactly the same as the single user space time coding scheme when there is no cooperation. When cooperation takes place, the destination observes a block fading channel [25, 26] since the links from U_1 and U_2 to the receiver are independent. When there is no cooperation, the destination observes a quasi-static fading channel. Similar to [24] and [23], each user uses a cyclic redundancy check (CRC) code for error detection along with a space time code for error correction.

A block diagram of the system is shown in Figure 2.9.

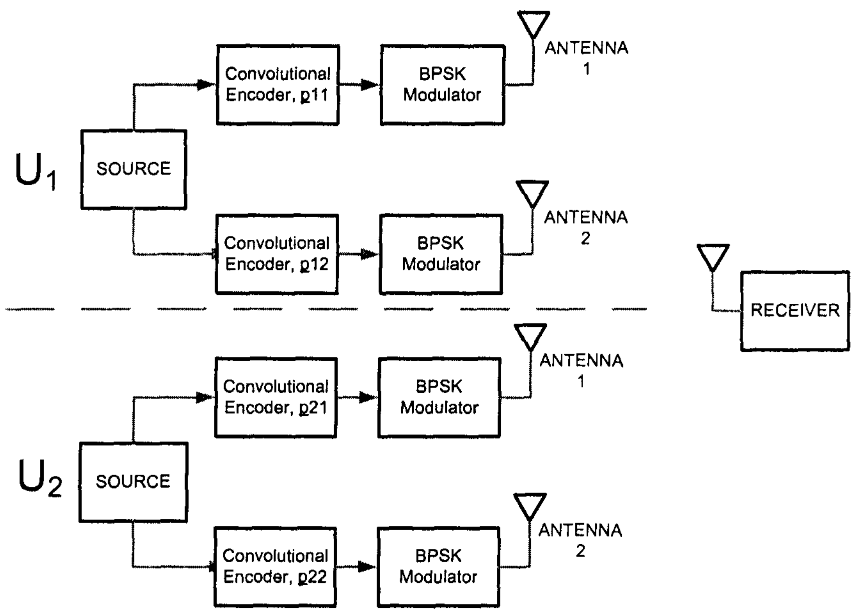

Figure 2.9: Block Diagram of the Model.

The information bits at each user, U_j (j = 1,2), are encoded by two convolutional encoders with generator polynomials $\{\underline{p}_{k,1}, \underline{p}_{k,2}\}$ (k = 1,2) where k denotes the segment index. The coded bits are then mapped to binary phase shift keying (BPSK) constellation. The output of the modulator from antenna i of segment k at time t is denoted by $c^k_{t,i}$. The coded bits from each user at time t are transmitted simultaneously from both antennas. The received signal r_t in the first segment at time t is given by

$$r_t = \sqrt{E_s}\sum_{i=1}^{2} g_{1,i}c_{t,i}^{1} + n_t \tag{2.5}$$

where $\{t = 1, 2, ..., L\}$ and L is the block length. When cooperation takes place, the received signal in the second segment is given by

$$r_t = \sqrt{E_s}\sum_{i=1}^{2} g_{2,i}c_{t,i}^{2} + n_t \tag{2.6}$$

where $\{t = L+1, L+2, ..., 2L\}$ and the noise over two segments, $\{n_t, t = 1, ..., 2L\}$, are outcomes of independent, zero-mean complex Gaussian r.v.'s with variance $\frac{N_0}{2}$ per dimension. When there is no cooperation, the received signal in the second segment is

$$r_t = \sqrt{E_s}\sum_{i=1}^{2} g_{1,i}c_{t,i}^{2} + n_t \tag{2.7}$$

with $\{t = L+1, L+2, ..., 2L\}$.

In [7], several suitable convolutional codes for cooperative space time coding that satisfy the algebraic design criteria in [25, 26] are obtained and shown in Table 2.1. The first column shows the constraint length K of the convolutional codes. The second column lists the generator polynomials used for U_1 at the first time second segment. The third column lists the generator polynomials used for the coded bits that either U_1 or U_2 transmits at the second time segment. Since each antenna transmits one encoded bit at a time using the corresponding rate 1 code for each user, the overall rate of the system is $\frac{1}{2}$.

A bound on the frame error rate (FER) of the cooperative space time coding system was proposed in [24] as

$$\begin{aligned} P_f^{Coop} &= (1 - P_f^{in})P_f^{BF} + P_f^{in}P_f^{QS} \\ &\leq P_f^{BF} + P_f^{in}P_f^{QS} \end{aligned} \tag{2.8}$$

where P_f^{in} denotes the FER of the inter-user channel, P_f^{BF} denotes the FER over the block fading channel when cooperation takes place, and P_f^{QS} denotes the FER over the

Table 2.1: Convolutional Codes Suitable for CSTC with Two Transmit Antennas at Each User in Octal Notation.

	U_1	U_2
K	p_{11} p_{12}	p_{21} p_{22}
3	5,7	5,7
4	15,17	13,15
5	23,35	25,37
6	53,75	67,71
7	133,171	117,165

quasi-static Rayleigh fading channel from the user to the receiver when there is no cooperation.

Suppose the probability that the receiver decides erroneously in favor of a signal

$$\mathbf{e} = e_{1,1}e_{1,2}...e_{1,m}e_{2,1}e_{2,2}...e_{2,m}...e_{L,1}e_{L,2}...e_{L,m} \tag{2.9}$$

assuming that

$$\mathbf{c} = c_{1,1}c_{1,2}...c_{1,m}c_{2,1}c_{2,2}...c_{2,m}...c_{L,1}c_{L,2}...c_{L,m} \tag{2.10}$$

was transmitted was considered where m denotes the number of transmit antennas. We can express the codeword difference matrix as

$$\mathbf{B(c,e)} = \begin{bmatrix} e_{1,1}-c_{1,1} & e_{2,1}-c_{2,1} & \cdots & \cdots & e_{L,1}-c_{L,1} \\ e_{1,2}-c_{1,2} & e_{2,2}-c_{2,2} & \cdots & \cdots & e_{L,2}-c_{L,2} \\ e_{1,3}-c_{1,3} & e_{2,3}-c_{2,3} & \cdots & \cdots & e_{L,3}-c_{L,3} \\ . & . & \cdots & . & . \\ e_{1,m}-c_{1,m} & e_{2,m}-c_{2,m} & \cdots & \cdots & e_{L,m}-c_{L,m} \end{bmatrix}. \tag{2.11}$$

Suppose we have m transmit antennas at each user and one receive antenna and assume all channels, including the inter-user channel, have the same quality ($E_{s_1} = E_{s_2} = E_{s_m} = E_s$).

using the pairwise error probability (PEP) expression (2) and (5) in [25], the union upper bound on the FER, (2.8) can be further expressed as

$$\begin{aligned} P_f^{Coop} &\leq P_f^{BF} + P_f^{in} P_f^{QS} \\ &\leq (\frac{E_s}{4N_0})^{-(2m)} \sum_{\mathbf{c}} \sum_{\mathbf{e} \neq c} \prod_{b=1}^{2} 1/\mu_b \\ &+ (\frac{E_s}{4N_0})^{-(2m+m)} (\sum_{\mathbf{c}} \sum_{\mathbf{e} \neq c} (\prod_{i=1}^{m} 1/\gamma_i)^m)(\sum_{\mathbf{c}} \sum_{\mathbf{e} \neq c} \prod_{i=1}^{m} 1/\lambda_i) \end{aligned} \tag{2.12}$$

where $\mu_1 = \prod_{i=1}^{m} \gamma_i$ and $\mu_2 = \prod_{i=1}^{m} \delta_i$ where γ_i and δ_i are the nonzero eigenvalues of $\mathbf{B}(\mathbf{c}, \mathbf{e})\mathbf{B}(\mathbf{c}, \mathbf{e})^{\mathbf{T}}$ for the fading block b = 1 and b = 2 respectively. It is assumed that the codeword-difference matrices in both fading blocks, b = 1, 2 are of full rank. Similarly, λ_i denotes the i^{th} nonzero eigenvalue of the product of the difference matrix and its conjugate transpose for the quasi-static channel [25].

It is shown in [14] that for a good inter-user channel, $P_f^{in} \approx 0$, $P_f^{Coop} \approx P_f^{BF}$,

$$P_f^{Coop} \approx \left(\kappa \frac{E_s}{4N_0}\right)^{-2m} \tag{2.13}$$

where κ denotes the most dominant term in the summation. This shows that when P_f^{in} is close to zero, cooperative space time coding achieves a diversity order of $2m$ with m antennas at each user.

Similarly, for a poor inter-user channel ($P_f^{in} \approx 1$), $P_f^{Coop} \approx P_f^{in} P_f^{QS}$, [14] assumed that $(E_{s_{in}}/4N_0)^{m^2} \leq C_{in}$ where C_{in} is a very small number due to the poor inter-user channel so that

$$P_f^{Coop} \approx \frac{1}{C_{in}} \left(\frac{E_s}{4N_0}\right)^{-m} \frac{1}{\Gamma} \tag{2.14}$$

where Γ denotes the minimum product of the codes eigenvalues which dominates the performance at high SNR. Hence, the maximum diversity order that the cooperative space time coding can achieve with poor inter-user channel is m [14].

Chapter 3

CSTC with Spatially Correlated Fading and Imperfect Channel Estimation

In this chapter, we obtain bounds on the performance of CSTC with convolutional encoding and BPSK modulation in spatially correlated Rayleigh fading with imperfect channel estimation. For clarity, we use uppercase letters to denote r.v.'s and the corresponding lowercase letters to denote their sample values.

3.1 System Model

Since the coded bits for the two segments are transmitted at different time and the channel gains are independent from user to user as in Section 2.5, we analyze the FER performance for the first segment with quasi-static fading and extend the analysis to block fading channel for cooperation. If there is no cooperation in the second time segment, the analysis is still valid since a quasi-static channel is equivalent to a block fading channel with same channel gains for each block. Within user j, the channel gains $G_{j,1}$ and $G_{j,2}$ are assumed to be independent (j = 1,2) in Section 2.5. However, in reality, insufficient antenna spacing may cause spatial correlations between antennas. In practice, most cellular communication systems require an antenna spacing of 50λ to 100λ at the base station [27] to ensure independency between antennas. In this section, we discuss the performance of CSTC when the channel gains are spatially correlated and when the channel estimation is not assumed to be perfect at the receiver.

Similar to the model used in Section 2.5, we use two transmit antennas at each user and one receive antenna at the destination. However, the two transmit antennas at each of the two users are close to each other and hence their channel gains are spatially correlated. The received signal at time t in segment 1 is given by

$$r_t = \sqrt{E_s}\sum_{i=1}^{2} g_{1,i}c_{t,i}^{1} + n_t \tag{3.1}$$

where the noise $\{n_t, t = 1, 2, ..., L\}$ are outcomes of independent, zero-mean complex Gaussian r.v. with variance $\frac{N_0}{2}$ per dimension and L denotes the block length. As mentioned in the discussion of block fading channel in Section 2.2, a frame consists of two blocks for CSTC model. The channel gains $G_{1,1}$ and $G_{1,2}$ are zero-mean complex Gaussian r.v.'s with variances σ_G^2 equal to 0.5 per dimension and are assumed to be constant within the transmission of one block. The term $c_{t,i}^{k}$ corresponds to the coded bit to be transmitted at time t from antenna i in segment k $(i, k = 1,2)$. The variance of a complex Gaussian r.v., i.e., X is defined as the variance of either its real or imaginary component and is denoted by σ_X^2 in this thesis. The real and imaginary parts are assumed to be independent. The channel gains are correlated for the two paths of each user but are independent from user to user. The correlation coefficient, ρ_s of $G_{1,1}$ and $G_{1,2}$ is

$$\rho_s = \frac{E[G_{1,1}G_{1,2}^{*}]}{\sqrt{E[|G_{1,1}|^2]E[|G_{1,2}|^2]}} \tag{3.2}$$

and the covariance matrix of $G_{1,1}$ and $G_{1,2}$ can be expressed as

$$\mathbf{C_G} = \begin{bmatrix} \sigma_G^2 & \rho_s\sigma_G^2 \\ \rho_s\sigma_G^2 & \sigma_G^2 \end{bmatrix} \tag{3.3}$$

In [14], the channel gains are assumed to be perfectly known at the receiver. In our model, the channel gains are to be estimated from the received signals. This can be done by using pilot symbol channel estimation [28] where a sample of the estimated channel gain from antenna 1 can be obtained as

$$\begin{aligned} h_{1,1} &= \frac{r_t}{\sqrt{E_s} c_{t,1}^1} \\ &= g_{1,1} + \frac{n_t}{\sqrt{E_s} c_{t,1}^1}. \end{aligned} \tag{3.4}$$

Let $z_{1,1} = \frac{n_t}{\sqrt{E_s} c_{t,1}^1}$ denotes the channel gain estimation error. Then $Z_{1,1}$ is a zero mean independent complex Gaussian r.v. with variance σ_Z^2 and $H_{1,1}$ is a zero mean complex Gaussian r.v. with variance

$$\sigma_{H_{1,1}}^2 = \sigma_{G_{1,1}}^2 + \sigma_{Z_{1,1}}^2 \tag{3.5}$$

Similarly, $\sigma_{H_{1,2}}^2 = \sigma_{G_{1,2}}^2 + \sigma_{Z_{1,2}}^2$. The system model for our performance analysis is shown in Figures 3.1 and 3.2.

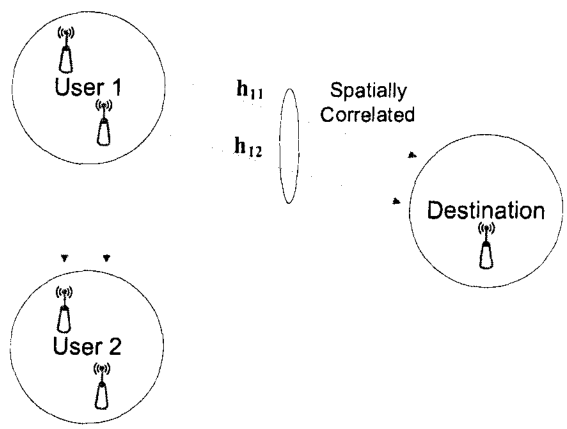

Figure 3.1: Modified Transmission Scheme : Segment 1.

Figures 3.1 and 3.2 explain the transmission of the two segments. The transmission scheme is the same as that described in Section 2.5 except the actual channel gains are replaced by $h_{1,i}$ and $h_{2,i}$ where $h_{1,i}$ and $h_{2,i}$ denote the estimated channel gains from antenna i of U_1 and U_2 to the destination $(i = 1, 2)$.

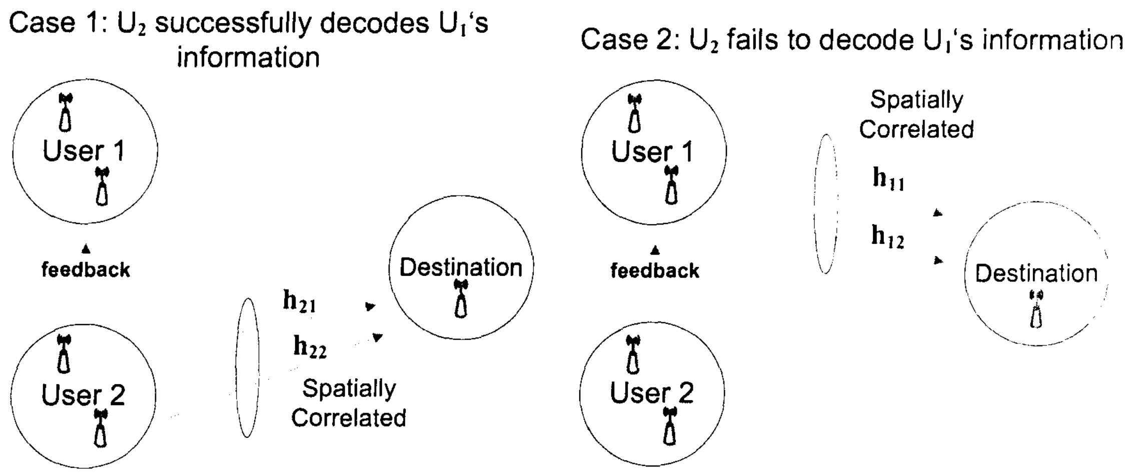

Figure 3.2: Modified Transmission Scheme : Segment 2.

The channel estimation error is assumed to be independent from antenna to antenna and independent of $G_{1,i}$, i.e.

$$E[Z_{1,i}Z_{1,j}^*] = E[G_{1,i}Z_{1,i}^*] = E[G_{1,i}Z_{1,j}^*] = 0, (i, j = 1, 2) \tag{3.6}$$

The correlation coefficient, ρ_e, between $G_{1,i}$ and $H_{1,i}$ is defined as

$$\rho_e = \frac{E[G_{1,i}H_{1,i}^*]}{\sqrt{E[|G_{1,i}|^2]E[|H_{1,i}|^2]}} = \frac{E[G_{1,i}(G_{1,i} + Z_{1,i})^*]}{\sqrt{(2\sigma_G^2)(2\sigma_H^2)}} = \frac{\sigma_G}{\sigma_H}. \tag{3.7}$$

It follows that

$$\sigma_H^2 = \frac{\sigma_G^2}{\rho_e^2} \tag{3.8}$$

and the variance of the channel estimator error can be expressed as

$$\sigma_Z^2 = (\frac{1}{\rho_e^2} - 1)\sigma_G^2. \tag{3.9}$$

Also, we have

$$E[H_{1,1}H_{1,2}^*] = E[(G_{1,1} + Z_{1,1})(G_{1,2} + Z_{1,2})^*] = 2\rho_s\sigma_G^2 \tag{3.10}$$

$$E[G_{1,1}H_{1,2}^*] = E[G_{1,1}(G_{1,2} + Z_{1,2})^*] = 2\rho_s\sigma_G^2 \tag{3.11}$$

$$E[G_{1,2}H_{1,1}^*] = E[G_{1,2}(G_{1,1} + Z_{1,1})^*] = 2\rho_s\sigma_G^2. \tag{3.12}$$

From (3.8) and (3.10), the covariance matrix of $H_{1,1}, H_{1,2}$ is

$$\mathbf{C_H} = \begin{bmatrix} \sigma_H^2 & \rho_s\sigma_G^2 \\ \rho_s\sigma_G^2 & \sigma_H^2 \end{bmatrix} = \begin{bmatrix} \frac{\sigma_G^2}{\rho_e^2} & \rho_s\sigma_G^2 \\ \rho_s\sigma_G^2 & \frac{\sigma_G^2}{\rho_e^2} \end{bmatrix}. \tag{3.13}$$

3.2 Performance Analysis Based on Estimated Channel Gains

In this section, we analyze the performance of the CSTC system by fixing the value of the inter-user FER, P_f^{in}, and deriving the cooperative FER , P_f^{Coop}, based on the expression in [14] where

$$P_f^{Coop} = (1 - P_f^{in})P_f^{BF} + P_f^{in}P_f^{QS}. \tag{3.14}$$

When the partner successfully decodes the user's information ($P_f^{in} = 0$), P_f^{Coop} reduces to the FER of the block fading channel. When the partner fails to decode the user's information ($P_f^{in} = 1$), P_f^{Coop} reduces to the FER of the quasi-static channel.

To determine the maximum likelihood (ML) decoding metric for the received signals given $H_{1,1}$ and $H_{1,2}$, we first find the joint pdf $G_{1,1}$ and $G_{1,2}$ given $H_{1,1}$ and $H_{1,2}$, $p_{G_{1,1},G_{1,2}|H_{1,1},H_{1,2}}(g_{1,1}, g_{1,2}|h_{1,1}, h_{1,2})$. From (3.3) and (3.13), the covariance matrix of $G_{1,1}$,$G_{1,2}$, $H_{1,1}$, and $H_{1,2}$ is

$$\mathbf{C_{GH}} = \begin{bmatrix} \sigma_G^2 & \rho_s\sigma_G^2 & \sigma_G^2 & \rho_s\sigma_G^2 \\ \rho_s\sigma_G^2 & \sigma_G^2 & \rho_s\sigma_G^2 & \sigma_G^2 \\ \sigma_G^2 & \rho_s\sigma_G^2 & \sigma_G^2/\rho_e^2 & \rho_s\sigma_G^2 \\ \rho_s\sigma_G^2 & \sigma_G^2 & \rho_s\sigma_G^2 & \sigma_G^2/\rho_e^2 \end{bmatrix} \tag{3.15}$$

and the joint pdf of $G_{1,1}, G_{1,2}, H_{1,1}, H_{1,2}$ can be written as

$$p_{G_{1,1},G_{1,2},H_{1,1},H_{1,2}}(g_{1,1},g_{1,2},h_{1,1},h_{1,2}) = \frac{1}{(2\pi)^2(\det(\mathbf{C_{GH}}))^{1/2}}\exp(-\frac{1}{2}\mathbf{X_{GH}^T}\mathbf{C_{GH}^{-1}}\mathbf{X_{GH}}) \tag{3.16}$$

where $\mathbf{X_{GH}^H} = [G_{1,1}\ G_{1,2}\ H_{1,1}\ H_{1,2}]$ and $\mathbf{C_{GH}^{-1}}$ is the inverse of the covariance matrix $\mathbf{C_{GH}}$

The pdf of $H_{1,1}$ and $H_{1,2}$ is

$$p_{H_{1,1},H_{1,2}}(h_{1,1},h_{1,2}) = \frac{1}{2\pi(\det(\mathbf{C_H}))^{1/2}}\exp(-\frac{1}{2}\mathbf{X_H^T}\mathbf{C_H^{-1}}\mathbf{X_H}) \tag{3.17}$$

where $\mathbf{X_H^H} = [H_{1,1}\ H_{1,2}]$ and $\mathbf{C_H}$ is given by (3.13).

Using (3.16) and (3.17), we can write the joint pdf of $G_{1,1}$,$G_{1,2}$ given $H_{1,1}$, $H_{1,2}$ as

$$\begin{aligned} & p_{G_{1,1},G_{1,2}|H_{1,1},H_{1,2}}(g_{1,1},g_{1,2}|h_{1,1},h_{1,2}) \\ = & \frac{p_{G_{1,1},G_{1,2},H_{1,1},H_{1,2}}(g_{1,1},g_{1,2},h_{1,1},h_{1,2})}{p_{H_{1,1},H_{1,2}}(h_{1,1},h_{1,2})} \\ = & \frac{1}{2\pi\sigma_D^2\sqrt{1-\rho_d^2}} \\ & \exp(-\frac{(g_{1,1}-m_{1,1})^2 - 2\rho_d(g_{1,1}-m_{1,1})(g_{1,2}-m_{1,2}) + (g_{1,2}-m_{1,2})^2}{2\sigma_D^2\sqrt{1-\rho_d^2}}) \end{aligned} \tag{3.18}$$

with

$$m_{1,1} = \frac{(h_{1,1}(1-\rho_s^2\rho_e^2) + h_{1,2}\rho_s(1-\rho_e^2))\rho_e^2}{1-\rho_s^2\rho_e^4} \tag{3.19}$$

$$m_{1,2} = \frac{(h_{1,2}(1-\rho_s^2\rho_e^2) + h_{1,1}\rho_s(1-\rho_e^2))\rho_e^2}{1-\rho_s^2\rho_e^4} \tag{3.20}$$

$$\sigma_D^2 = \frac{\sigma_G^2(1-\rho_e^2)(1-\rho_s^2\rho_e^2)}{1-\rho_s^2\rho_e^4} \tag{3.21}$$

$$\rho_d = \frac{\rho_s(1-\rho_e^2)}{1-\rho_s^2\rho_e^2} \tag{3.22}$$

As in [11], we can express $g_{1,1}$, $g_{1,2}$ in terms of $h_{1,1}$, $h_{1,2}$ as

$$g_{1,1} = m_{1,1} + d_{1,1} = ah_{1,1} + bh_{1,2} + d_{1,1} \tag{3.23}$$

$$g_{1,2} = m_{1,2} + d_{1,2} = bh_{1,1} + ah_{1,2} + d_{1,2} \tag{3.24}$$

where

$$a = \frac{\rho_e^2(1-\rho_s^2\rho_e^2)}{1-\rho_s^2\rho_e^4} \tag{3.25}$$

$$b = \frac{\rho_e^2\rho_s(1-\rho_e^2)}{1-\rho_s^2\rho_e^4} \tag{3.26}$$

and $D_{1,1}$ and $D_{1,2}$ are zero mean correlated complex Gaussian with variance σ_D^2 and correlation coefficient ρ_d. The received vector for the first time segment can then be expressed as

$$\begin{aligned} r_t &= \sqrt{E_s}g_{1,1}c_{t,1}^1 + \sqrt{E_s}g_{1,2}c_{t,2}^1 + n_t \\ &= \sqrt{E_s}m_{1,1}c_{t,1}^1 + \sqrt{E_s}m_{1,2}c_{t,2}^1 + \sqrt{E_s}d_{1,1}c_{t,1}^1 + \sqrt{E_s}d_{1,2}c_{t,2}^1 + n_t \end{aligned} \tag{3.27}$$

With (3.19) to (3.22), R_t given $H_{1,1}$ and $H_{1,2}$ can be written as [1]

$$\begin{aligned} p_{R_t|H_{1,1},H_{1,2}}(r_t|h_{1,1},h_{1,2}) &= \frac{p_{R_t,H_{1,1},H_{1,2}}(r_t,h_{1,1},h_{1,2})}{p_{H_{1,1},H_{1,2}}(h_{1,1},h_{1,2})} \\ &= \frac{1}{\sqrt{2\pi\sigma^2_{R_t|H_{1,1},H_{1,2}}}}\exp\left(-\frac{1}{2}\frac{|r_t-\mu|^2}{\sigma^2_{R_t|H_{1,1},H_{1,2}}}\right) \end{aligned} \tag{3.28}$$

where

$$\mu = \sqrt{E_s}\sum_{i=1}^{2} m_{1,i}c_{t,i}^1 \tag{3.29}$$

$$\sigma^2_{R_t|H_{1,1},H_{1,2}} = E_s\frac{(1-\rho_e^2)(1-\rho_s^2\rho_e^2)}{1-\rho_s^2\rho_e^4} + 2E_sc_{t,1}^1c_{t,2}^1\rho_d\sigma_D^2 + \frac{N_0}{2}. \tag{3.30}$$

For the case where the channel gains with each user are independent, i.e. $\rho_s = 0$, (3.29) and (3.30) reduce to

$$\mu = \sqrt{E_s}\rho_e^2\sum_{i=1}^{2} h_{1,i}c_{t,i}^1 \tag{3.31}$$

$$\sigma^2_{R_t|H_{1,1},H_{1,2}} = E_s(1-\rho_e^2) + \frac{N_0}{2} \tag{3.32}$$

, which are the same results as shown in [31].

Suppose a codeword

$$\mathbf{c} = c_{1,1}^1 c_{1,2}^1 c_{2,1}^1 c_{2,2}^1 \ldots c_{L,1}^1 c_{L,2}^1 \tag{3.33}$$

is sent in segment 1 and the received vector is

$$\mathbf{r} = r_1 \ r_2 \ r_3 \ldots r_L \tag{3.34}$$

where L denotes the block length. Optimum decoding amounts to choosing a codeword

$$\mathbf{e} = e_{1,1}^1 e_{1,2}^1 e_{2,1}^1 e_{2,2}^1 \ldots e_{L,1}^1 e_{L,2}^1 \tag{3.35}$$

for which the likelihood $P(\mathbf{r}|\mathbf{e}, H_{1,1} = h_{1,1}, H_{1,2} = h_{1,2})$ is maximized. The components of the received vector, $\mathbf{r}$ given the estimated channel gains are assumed to be independent in [29]. However, it is noted in [30] that this assumption is mathematically inaccurate. Since no explanation was given in [30], a discussion of this dependency is given in Appendix B.

We assume that the elements of the received vector, $\mathbf{r}$, are independent in order to obtain a closed form analytical bound which is then compared with our simulation results. Taking the logarithm of the likelihood $P(\mathbf{r}|\mathbf{e}, H_{1,1} = h_{1,1}, H_{1,2} = h_{1,2})$, we decide in favor of the codeword $\mathbf{e}$ which minimizes the quantity

$$\sum_{t=1}^{L} -\log P(r_t | e_{t,1}^1 \ e_{t,2}^1, H_{1,1} = h_{1,1}, H_{1,2} = h_{1,2}). \tag{3.36}$$

From (3.36), the decoder chooses $\mathbf{e}$ to minimize

$$\begin{aligned} &\sum_{t=1}^{L} \Big(\frac{|r_t - \sqrt{E_s} \sum_{i=1}^{2} e_{t,i}^1 m_i|^2}{N_0 + 4E_s e_{t,1}^1 e_{t,2}^1 \rho_d \sigma_D^2 + 2E_s \frac{(1-\rho_e^2)(1-\rho_s^2\rho_e^2)}{1-\rho_s^2\rho_e^4}} \\ + \ & \frac{1}{2} \ln \left(\pi N_0 + 4\pi E_s e_{t,1}^1 e_{t,2}^1 \rho_d \sigma_D^2 + 2\pi E_s \frac{(1-\rho_e^2)(1-\rho_s^2\rho_e^2)}{1-\rho_s^2\rho_e^4} \right) \Big). \end{aligned} \tag{3.37}$$

For the case where the channel estimation is not very poor ($\rho_e \approx 0.99$), we can assume that $2E_s e_{t,1}^1 e_{t,2}^1 \rho_d \sigma_D^2 \approx 0$

Thus, by dropping the constant terms,(3.37) can be simplified as

$$\sum_{t=1}^{L}\left|r_t - \sqrt{E_s}\sum_{i=1}^{2} e_{t,i}^{1} m_{1,i}\right|^2 . \tag{3.38}$$

A frame error occurs when

$$\sum_{t=1}^{L}|r_t - \sqrt{E_s}\sum_{i=1}^{2} c_{t,i}^{1} m_{1,i}|^2 > \sum_{t=1}^{L}|r_t - \sqrt{E_s}\sum_{i=1}^{2} e_{t,i}^{1} m_{1,i}|^2 \tag{3.39}$$

Expanding (3.39) and we get

$$\begin{aligned} X &= r_t\sqrt{E_s}\sum_{i=1}^{2} m_{1,i}^{*}(e_{t,i}^{1} - c_{t,i}^{1}) + r_t^{*}\sqrt{E_s}\sum_{i=1}^{2} m_{1,i}(e_{t,i}^{1} - c_{t,i}^{1}) \\ &+ \sqrt{E_s}^2|\sum_{i=1}^{2} m_{1,i}c_{t,i}^{1}|^2 - \sqrt{E_s}^2|\sum_{i=1}^{2} m_{1,i}e_{t,i}^{1}|^2 > 0 \end{aligned} \tag{3.40}$$

where X given $H_{1,1}$ and $H_{1,2}$ is a real Gaussian with mean and variance as

$$\mu_X = -E_s L|\sum_{i=1}^{2} m_{1,i}(c_{t,i}^{1} - e_{t,i}^{1})|^2 \tag{3.41}$$

$$\sigma_X^2 = 2\sigma_{R_t|H_{1,1},H_{1,2}}^2 E_s L^2|\sum_{i=1}^{2} m_{1,i}(c_{t,i}^{1} - e_{t,i}^{1})|^2 . \tag{3.42}$$

Hence, the probability of $X|H_{1,1}, H_{1,2}$ greater than zero is

$$\begin{aligned} \Pr\{X|H_{1,1}, H_{H1,2} > 0\} &= Q\left(\sqrt{\frac{\mu_X^2}{\sigma_X^2}}\right) \\ &= Q\left(\sqrt{\frac{E_s}{2N_0 + 4E_s\frac{(1-\rho_e^2)(1-\rho_s^2\rho_e^2)}{1-\rho_s^2\rho_e^4}}d^2(\mathbf{c},\mathbf{e})}\right) \end{aligned} \tag{3.43}$$

with

$$d^2(\mathbf{c},\mathbf{e}) = \sum_{t=1}^{L}|\sum_{i=1}^{2} m_{1,i}(c_{t,i}^{1} - e_{t,i}^{1})|^2 . \tag{3.44}$$

From (3.38) to (3.44), we can easily extend the quasi-static analysis to block fading where the probability of deciding in favor of $\mathbf{e}$ given the estimated channel gains for CSTC with spatially correlated fading and imperfect channel estimation error over two segments is

$$
\begin{aligned}
& P(\mathbf{c} \to \mathbf{e} | H_{j,i} = h_{j,i}, i, j = 1, 2) \\
= \; & Q\left(\sqrt{\frac{E_s}{2N_0 + 4E_s \frac{(1-\rho_e^2)(1-\rho_s^2\rho_e^2)}{1-\rho_s^2\rho_e^4}} d^2(\mathbf{c}, \mathbf{e})}\right)
\end{aligned} \tag{3.45}
$$

with

$$
d^2(\mathbf{c}, \mathbf{e}) = \sum_{b=1}^{B} \sum_{t=1}^{L} |\sum_{i=1}^{2} m_{b,i}(c_{t,i}^b - e_{t,i}^b)|^2 \tag{3.46}
$$

and B refers to the number of blocks in the proposed model. The number of blocks for the block fading channel model used in the thesis is equivalent to the number of time segments used for coded bits transmission as in Figures 3.1 and 3.2. It is assumed that the derived closed form PEP conditioned on the estimated channel gains assuming the elements of the received vector are independent is an Upper Bound to the actual simulation.

For the case with imperfect channel estimation (i.e. $\rho_e \neq 1$), independent channels (i.e. $\rho_s = 0$), and B = 1, (3.45) and (3.46) reduce to

$$
P(\mathbf{c} \to \mathbf{e} | H_i = h_i, i = 1, 2) = Q\left(\sqrt{d^2(\mathbf{c}, \mathbf{e}) \rho_e^4 \frac{E_s}{2N_0 + 4E_s(1 - \rho_e^2)}}\right) \tag{3.47}
$$

with

$$
d^2(\mathbf{c}, \mathbf{e}) = \sum_{t=1}^{L} |\sum_{i=1}^{2} h_i(c_{t,i} - e_{t,i})|^2, \tag{3.48}
$$

which is the same result as shown in [31] for space time trellis codes with imperfect channel estimation.

For the case with perfect channel estimation at the receiver (i.e. $\rho_e = 1$), independent channels among each user (i.e. $\rho_s = 0$), and B = 1, (3.45) and (3.46) reduce to

$$
P(\mathbf{c} \to \mathbf{e} | G_i = g_i, i = 1, 2) = Q\left(\sqrt{\frac{E_s}{2N_0} d^2(\mathbf{c}, \mathbf{e})}\right) \tag{3.49}
$$

with

$$d^2(\mathbf{c}, \mathbf{e}) = \sum_{t=1}^{L} |\sum_{i=1}^{2} g_i(c_{t,i} - e_{t,i})|^2, \tag{3.50}$$

which is the same result as shown in [4] for perfect channel estimation and independent channel gains.

3.3 Evaluation of Expurgated Union Bound with Limiting Before Averaging Technique

In the standard union bound technique, we get

$$P_f \leq \int_{\mathbf{H}} \frac{1}{|\mathbf{S}|} \sum_{\mathbf{c}} \sum_{\mathbf{e} \neq \mathbf{c}} P(\mathbf{c} \to \mathbf{e} | \mathbf{H} = \mathbf{h}) \mathbf{p}_{\mathbf{H}}(\mathbf{h}) d\mathbf{h} \tag{3.51}$$

where $\mathbf{H}$ denotes the vector of estimated channel gains, $\mathbf{p}_{\mathbf{H}}(\mathbf{h})$ is the joint probability density function of $\mathbf{H}$ obtained in (3.17), and $|\mathbf{S}|$ denotes the total number of codewords in the space time code, which is 2^L.

As shown in [32], the union bound evaluated in a straight forward manner is quite loose for quasi-static, or block fading channels. Following [33], we will tighten the bound by performing expurgation of the standard union bound and use the limit before averaging technique proposed in [32] where we limit the conditional union upper bound on the error probability before averaging over the fading distribution. The expurgated union bound with limit before averaging technique is

$$\begin{aligned} P_f &\leq \int_{\mathbf{H}} \min \left[1, \frac{1}{|\mathbf{S}|} \sum_{\mathbf{c}} \sum_{\mathbf{e} \neq \mathbf{c}} P(\mathbf{c} \to \mathbf{e} | \mathbf{H}) \right] p_{\mathbf{H}}(\mathbf{h}) d\mathbf{h} \\ &\leq \int_{\mathbf{H}} \min \left[1, \frac{1}{|\mathbf{S}|} \sum_{\mathbf{c}} \sum_{\mathbf{e} \neq \mathbf{c}} Q \left(\sqrt{\frac{E_s}{2N_0 + 4E_s \frac{(1-\rho_e^2)(1-\rho_s^2\rho_e^2)}{1-\rho_s^2\rho_e^4}} d^2(\mathbf{c}, \mathbf{e})} \right) \right] p_{\mathbf{H}}(\mathbf{h}) d\mathbf{h} \end{aligned} \tag{3.52}$$

where $P(\mathbf{c} \to \mathbf{e}|\mathbf{H})$ corresponds to the expression derived in (3.45). The distance term, $d^2_{BF}(c, e)$ for P_f^{BF} is

$$\begin{aligned} d^2_{BF}(c, e) &= \sum_{b=1}^{2} |m_{b,1}|^2 A^1_{b,1} + \sum_{b=1}^{2} |m_{b,2}|^2 A^2_{b,2} \\ &+ 2\Re\{\sum_{b=1}^{2}(m_{b,1}m^*_{b,2})B_b\} \end{aligned} \tag{3.53}$$

where B corresponds to the number of blocks (segments) and

$$A^1_{b,1} = \sum_{t=1}^{L} |(c^b_{t,1} - e^b_{t,1})|^2 \tag{3.54}$$

$$A^2_{b,2} = \sum_{t=1}^{L} |(c^b_{t,2} - e^b_{t,2})|^2 \tag{3.55}$$

$$B_b = \sum_{t=1}^{L} (c^b_{t,1} - e^b_{t,1})(c^b_{t,2} - e^b_{t,2})^*. \tag{3.56}$$

The distance term, $d^2_{QS}(c, e)$ for P_f^{QS} is

$$\begin{aligned} d^2_{QS}(c, e) &= 2|m_{1,1}|^2 A^1_1 + 2|m_{1,2}|^2 A^2_2 \\ &+ 2\Re\{2(m_{1,1}m^*_{1,2})B\} \end{aligned} \tag{3.57}$$

where

$$A^1_1 = \sum_{t=1}^{L} |(c_{t,1} - e_{t,1})|^2 \tag{3.58}$$

$$A^2_2 = \sum_{t=1}^{L} |(c_{t,2} - e_{t,2})|^2 \tag{3.59}$$

$$B = \sum_{t=1}^{L} (c_{t,1} - e_{t,1})(c_{t,2} - e_{t,2})^*. \tag{3.60}$$

Detail explanations about the extended trellis and the distance terms resulted from the expurgation technique are shown in Appendix B.

Chapter 4

Comparison of Analytical and Simulated Results

For illustration purposes, we consider BPSK modulation and the constraint length 3, four-state cooperative space time trellis code in Table 2.1 with a frame size of 260 bits. Examples with a higher number of states were also simulated. However, only analytical results for a constraint length 3 code were obtained because the size of the expurgated transition matrix for codes with a higher number of states is too big. (See Appendix B for a discussion of the complexity)

4.1 FER Comparison

The analytical Upper Bounds (UBs) and simulated FER curves are plotted as a function of the SNR for different (ρ_s ρ_e) values. By increasing ρ_s, the channel gains between the two transmit antennas with each user become more correlated whereas the estimates of the channel gains get worse with decreasing ρ_e. The SNR is defined as the ratio of the variance of the complex channel gains to the variance of the additive Gaussian noise, i.e., $\frac{\sigma_G^2}{\sigma_N^2}$, or $\frac{2E_s}{N_0}$ as in Appendix C. Analytical and simulated FER curves for two extreme cases: SUSTC ($P_f^{in} = 1$) and CSTC ($P_f^{in} = 0$) with spatially correlated fading and imperfect channel estimations are presented where P_f^{in} denotes the FER of the inter-user channel between users.

4.1.1 Single User Space Time Coding (SUSTC)

The FER performance of the SUSTC with different (ρ_e ρ_s) values is discussed in this section. The simulation results are then compared with the corresponding UB curves.

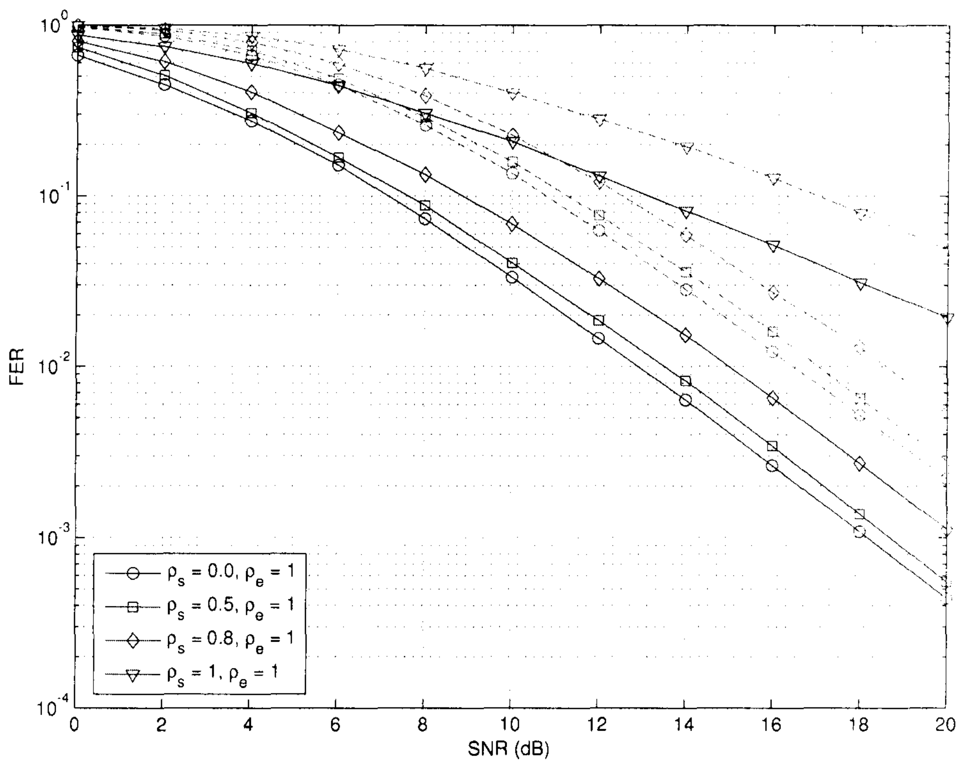

Figure 4.1: Comparison of Analytical and Simulation Results for Single User Space Time Coding with fixed ρ_e at 1 and varying ρ_s : BPSK modulation, (5, 7, 5, 7) convolutional code (upper bound: dashed lines; simulation: solid lines)

In [33], the FER performance of the 4-PSK, four-state space time trellis codes proposed in [4] with two transmit and one receive antennas over spatially correlated quasi-static fading channels with perfect channel estimation and a frame size of 130 symbols was analyzed. It was observed in [33] that the UB captures the diversity and accurately predicts the performance of the space time trellis codes and is about 3.5 dB away from the results obtained through simulation. As for the SUSTC model proposed in the thesis, full diversity order was achieved with perfect channel estimation (ρ_e = 1) and independent quasi-static Rayleigh fading channels ($\rho_s = 0$) as in Figure 4.1. Diversity order is defined as the gradient of the performance curve as SNR approaches infinity. It is observed that the FER increases as ρ_s increases from 0 to 1 with $\rho_e = 1$. From the simulation curves at a target FER of 10^{-1}, there is about 0.5 dB degradation when ρ_s increases from 0 to 0.5 and about 1.8 dB degradation when ρ_s increases from 0 to 0.8. The degradation grows to 6 dB as ρ_s increases from 0 to 1. From the analytical UB curves, we observe that the expurgated UBs with limiting before averaging technique [32] are about 3.5 to 4 dB away from the corresponding simulation curves. Even though the bound is loose, it captures the FER degradations of the simulation results nicely as the degradations are about 0.47, 1.7 and 6.1 dB as ρ_s increases from 0 to 0.5, 0.8 and 1 respectively.

Figure 4.2 shows the FER performance of SUSTC with different ρ_s values and $\rho_e = 0.99$. It is observed that the FER increases as ρ_s increases from 0 to 1 with $\rho_e = 0.99$. For a target FER at 10^{-1}, the simulation curve shows a 0.67 dB degradation when ρ_s increases from 0 to 0.5 and a 2.2 dB degradation when ρ_s increases from 0 to 0.8. The degradation grows to 6.3 dB as ρ_s increases from 0 to 1 when the two channel gains are fully correlated within each user. The FER degradations for the UB curves are 0.73, 2.5, and 8.1 dB as ρ_s increases from 0 to 0.5, 0.8, and 1 respectively. If ρ_e continues to decrease to 0.9 as shown in Figure 4.3, the target FER of 0.1 cannot be achieved. It is shown in Figure 4.3 that with $\rho_e = 0.9$, as ρ_s increases to 1, the simulated FER outperforms the cases with ρ_s = 0, 0.5, and 0.8 at high SNR and a performance reversal occurs when ρ_s increases from 0.8 to 1 in the UB curves. A possible explanation for this is as $\rho_s \rightarrow 1$, the probability of both channels are good is higher. When both channels are good, the probability of decoding the frame more correctly is higher.

From Figures 4.1, 4.2, and 4.3, the FER curves exhibit a floor. The floors represent the best performance that SUSTC can achieve given the corresponding ρ_e value. The analytical expression for the floor can be obtained from (3.47) and (3.52) with the distance term equal to (3.57). Generally, it is observed from Figures 4.1, 4.2, and 4.3 that the FER increases as ρ_s increases from 0 to 1 and as ρ_e decreases from 1 to 0. For ρ_e

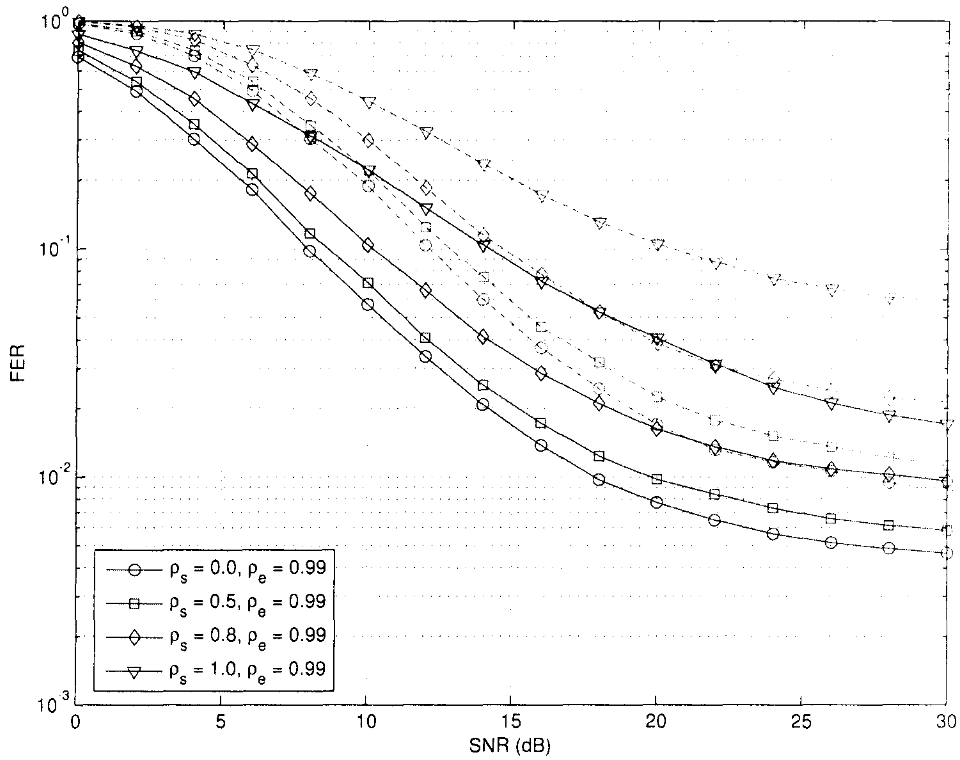

Figure 4.2: Comparison of Analytical and Simulation Results for Single User Space Time Coding with fixed ρ_e at 0.99 and varying ρ_s : BPSK modulation, (5, 7, 5, 7) convolutional code (upper bound: dashed lines; simulation: solid lines)

= 1, the FER degradations match well with the simulation results with increasing ρ_s. However, the degradations between the analytical and simulation results are different when ρ_e decreases to 0.99 because the UB curves have higher floors which cause the UB curves to reach the flattening part faster at the target FER. Similar to [11] where the BER performance analysis of Alamouti coding with spatially correlated Rayleigh fading and channel estimation error was presented, it can be observed that spatial correlation causes the FER performance to degrade more as the channel estimation error increases. For a target FER of 10^{-1} and $\rho_e = 1$, the degradations are about 0.5 and 1.8 as ρ_s increases from 0 to 0.5 and 0.8 respectively. When $\rho_e = 0.99$, the degradations increase to 0.67 and 2.2 dB respectively.

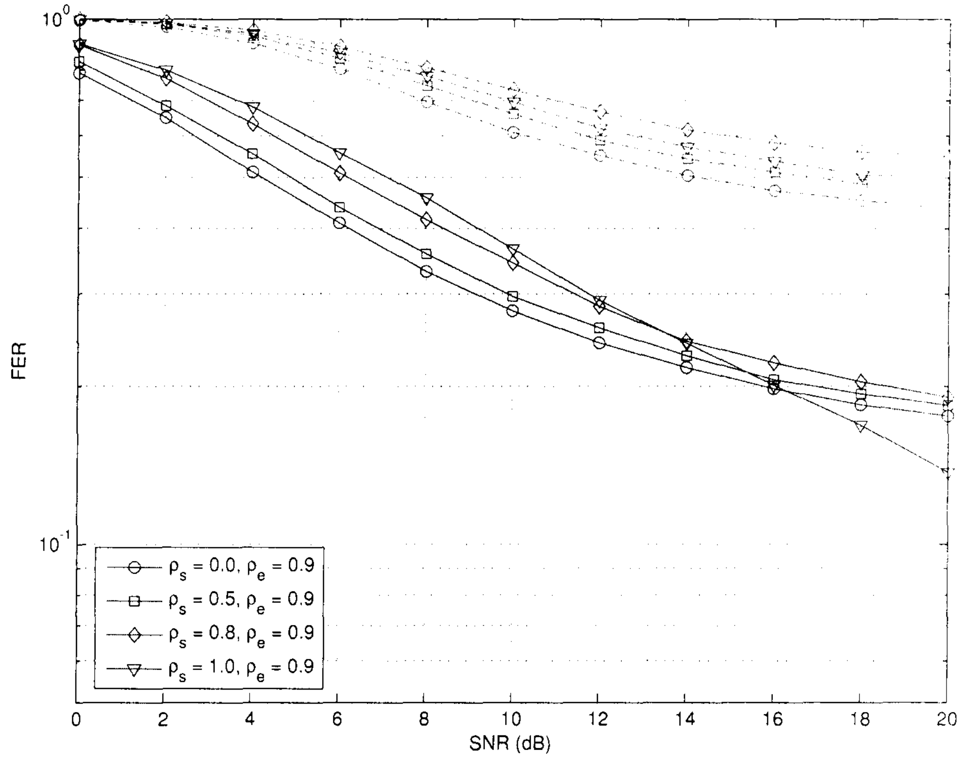

Figure 4.3: Comparison of Analytical and Simulation Results for Single User Space Time Coding with fixed ρ_e at 0.9 and varying ρ_s : BPSK modulation, (5, 7, 5, 7) convolutional code (upper bound: dashed lines; simulation: solid lines)

4.1.2 Cooperative Space Time Coding (CSTC)

The FER performance of the CSTC with different (ρ_e ρ_s) values is discussed in this section. The simulation results are then compared with the corresponding UB curves.

In [34], the FER performance of the 4-PSK, four-state space-time trellis code proposed in [4] with two transmit and two receive antennas over independent block fading channels with a frame size of 520 symbols was analyzed. Full diversity order was able to be achieved with the given codes. As shown in Figure 4.4, CSTC with perfect channel estimation ($\rho_e = 1$) proposed in the thesis achieves full diversity order over the independent block Rayleigh fading channels ($\rho_s = 0$) and the FER performance degrades with increasing ρ_s.

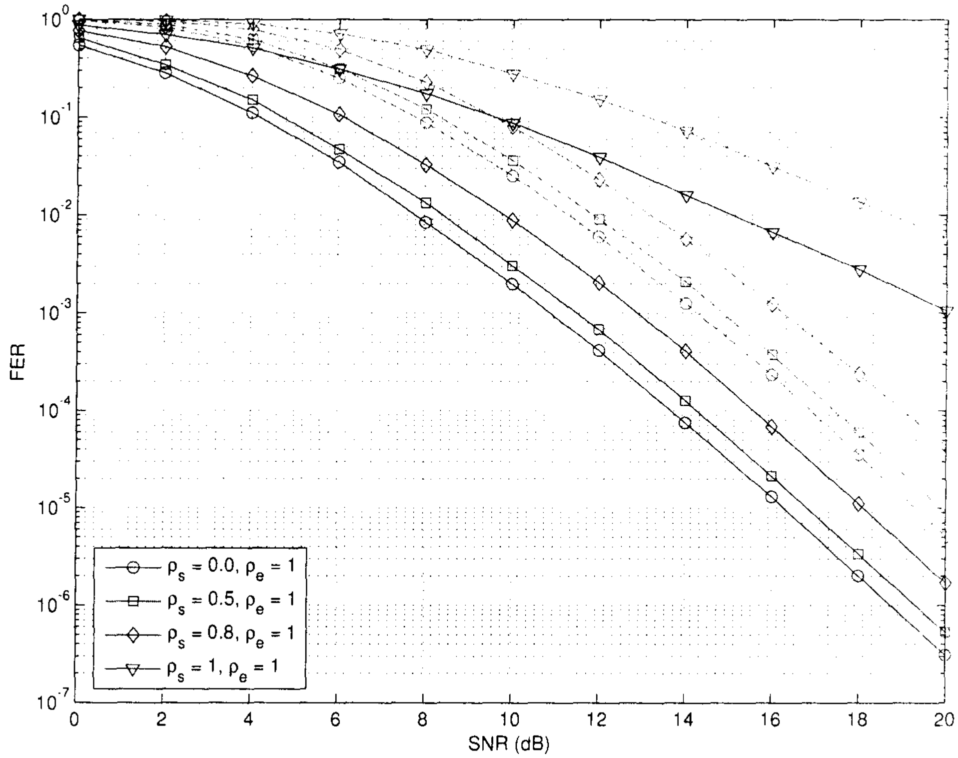

Figure 4.4: Comparison of Analytical and Simulation Results for Cooperative Space Time Coding with fixed ρ_e at 1 and varying ρ_s : BPSK modulation, (5, 7, 5, 7) convolutional code (upper bound: dashed lines; simulation: solid lines)

From the simulation curves at a target FER of 10^{-2}, there is about 0.6 dB degradation when ρ_s increases from 0 to 0.5 and about 2.0 dB degradation when ρ_s increases from 0 to 0.8. The degradation grows to 7.3 dB as ρ_s increases to 1. From the analytical UB curves, we observe that the expurgated UBs with the limiting before averaging technique [32] are about 3.5 to 4 dB away from the corresponding simulation curves. The degradations for the UB curves as ρ_s increases match well with the simulation curves. As ρ_s increases from 0 to 0.5, 0.8 and 1, the degradations for the UB curves are 0.6, 2.0, and 7.5 dB respectively.

Figure 4.5 shows the FER performance of the simulation and UB curves with $\rho_e = 0.99$ and different values of ρ_s. As ρ_e decreases from 1 to 0.99, with a target FER at 10^{-2},

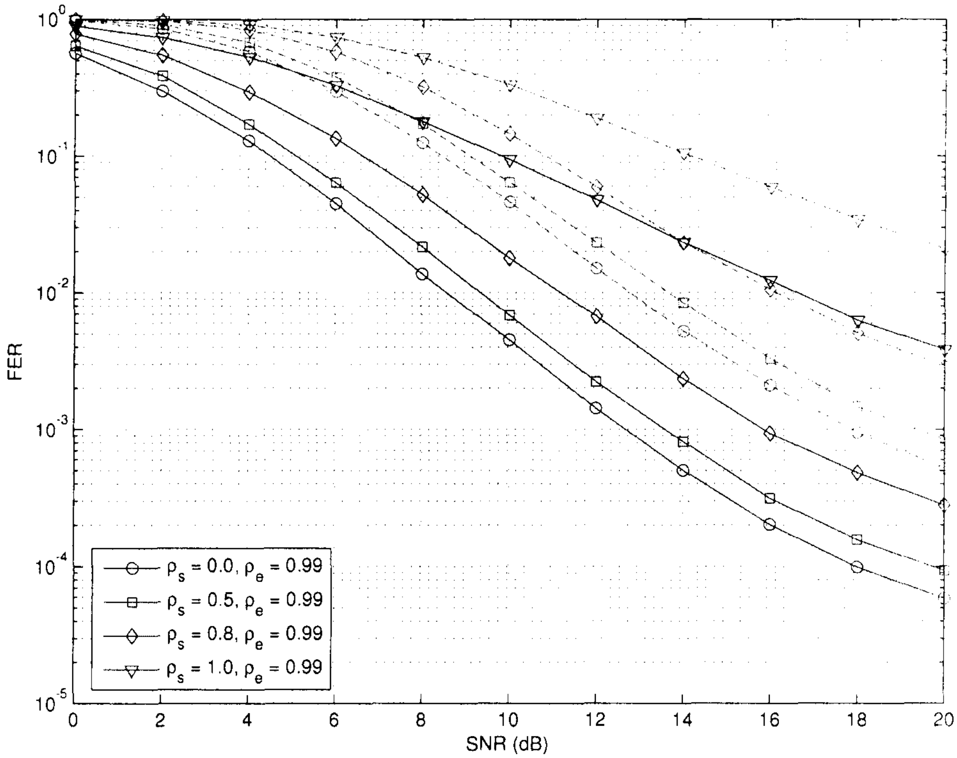

Figure 4.5: Comparison of Analytical and Simulation Results for Cooperative Space Time Coding with fixed ρ_e at 0.99 and varying ρ_s : BPSK modulation, (5, 7, 5, 7) convolutional code (upper bound: dashed lines; simulation: solid lines)

there is about 0.68 dB degradation when ρ_s increases from 0 to 0.5 and about 2.5 dB degradation when ρ_s increases from 0 to 0.8. When ρ_s increases from 0 to 1, the degradation grows to 8 dB. The degradations for the UB curves are 0.9 and 3.3 dB as ρ_s increases from 0 to 0.5 and 0.8 respectively. When ρ_s increases to 1, the degradation can not be observed as the target FER cannot be obtained. If ρ_e continues to decrease, ie. 0.9, as shown in Figure 4.6, the target FER of 0.01 cannot be achieved. Similar to the SUSTC with $\rho_e = 0.9$, as ρ_s increases to 1, the simulated FER of CSTC outperforms the case where $\rho_s = 0$, 0.5, and 0.8 at high SNR and a performance reversal occurs as ρ_s increases from 0.8 to 1 in the analytical UB curves. Possible explanation for this because as $\rho_s \to 1$, the probability of both channels within U_1 and U_2 are good is higher. Thus, the probability of decoding the frame more correctly is higher.

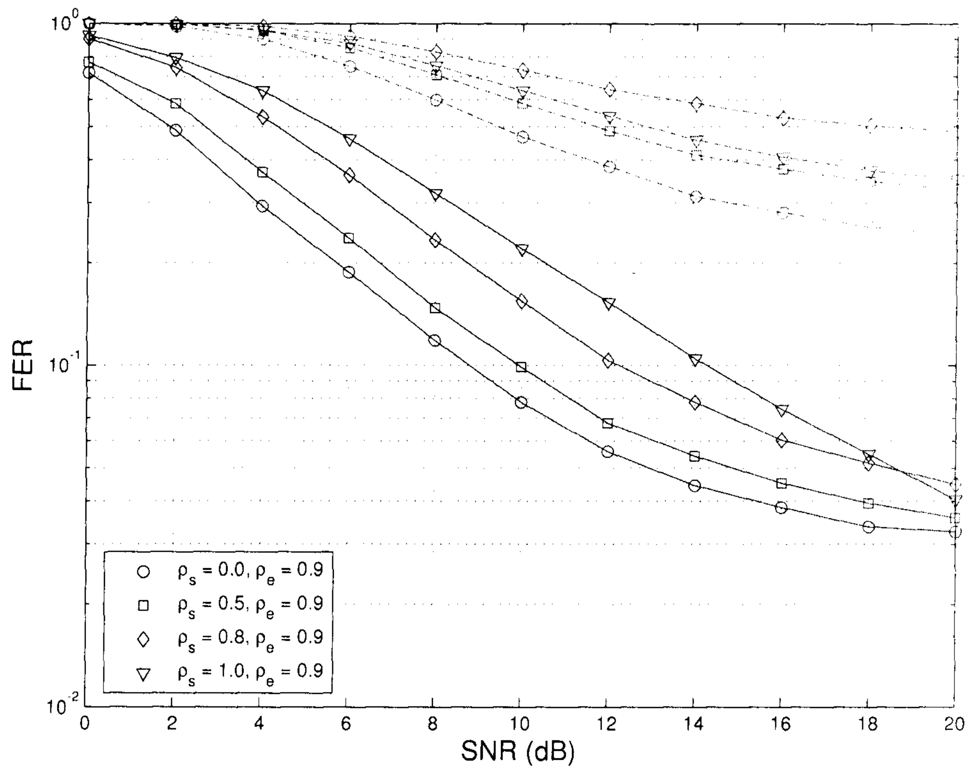

Figure 4.6: Comparison of Analytical and Simulation Results for Cooperative Space Time Coding with fixed ρ_e at 0.9 and varying ρ_s : BPSK modulation, (5, 7, 5, 7) convolutional code

A performance floor for CSTC can also be obtained at $\rho_s = 0$ as shown in Figures 4.4, 4.5, and 4.6. The floors represent the best performance that CSTC can achieve at a given ρ_e value. The analytical UBs for the performance floor can be obtained from (3.47) and (3.52) with the distance term equal to (3.53). Generally, it is observed from Figures 4.4, 4.5, and 4.6 that the FER increases as ρ_s increases from 0 to 1 and as ρ_e decreases from 1 to 0. Similar to SUSTC, it can be observed that spatial correlation causes the FER performance to degrade more as the channel estimation error increases. For a target FER of 10^{-2} and $\rho_e = 1$, the degradations are about 0.6 and 2.0 as ρ_s increases from 0 to 0.5 and 0.8 respectively. When $\rho_e = 0.99$, the degradations increase to 0.68 and 2.5 dB.

4.1.3 Comparison of SUSTC and CSTC

The simulated FER curves for SUSTC and CSTC with spatially correlated fading and perfect channel estimation are presented in this section.

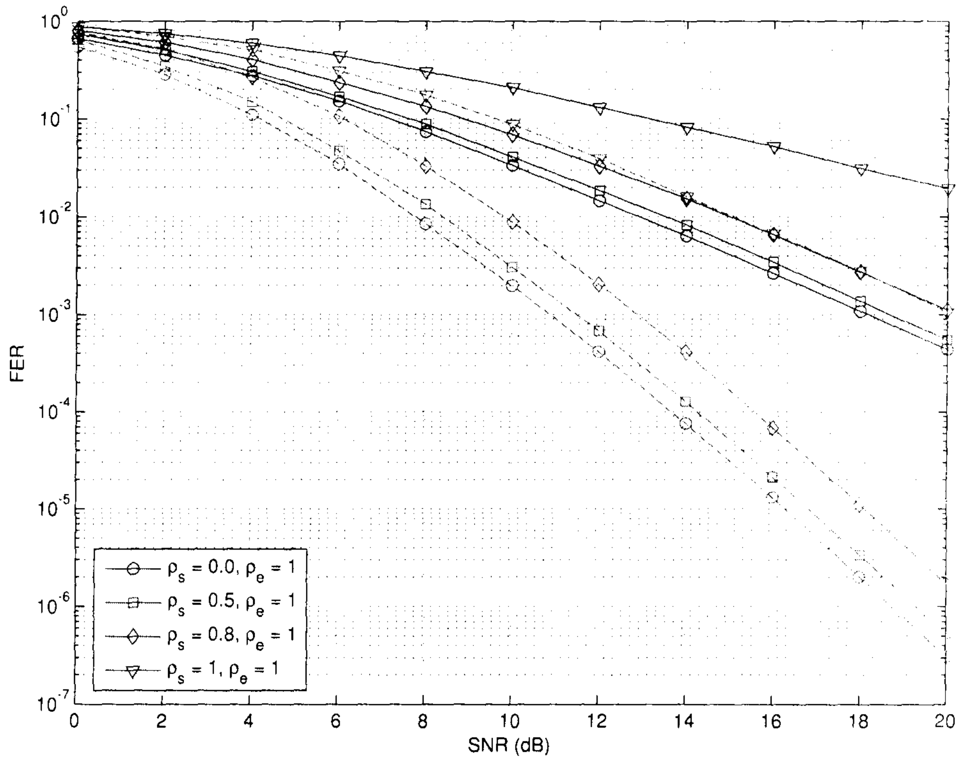

Figure 4.7: Comparison of the Simulation Results for Single User and Cooperative Space Time Coding at ρ_e at 1 and different values of ρ_s (Cooperation: dashed lines; Single User: solid lines)

Figure 4.7 shows the FER curves for SUSTC and CSTC as a function of SNR for different values of ρ_s with $\rho_e = 1$. It is observed that at high SNR, the diversity order for SUSTC and CSTC are approximated to be 2 and 4 respectively for ρ_s equal to 0, 0.5, and 0.8. In particular, the diversity orders for SUSTC and CSTC obtained for $\rho_s = 0$ confirm with the analysis shown at the end of Chapter 2 where the expected diversity order for SUSTC is equal to the number of transmit antennas (2 in the thesis) at each user whereas the expected diversity order for CSTC is equal to the sum of the number of transmit antennas for both users (4 in the thesis) [14]. When ρ_s increases to 1 (i.e. the two channels are fully correlated), independent fading paths can no longer be assumed within each user. Thus, the diversity orders decrease to 1 and 2 for SUSTC and CSTC respectively.

4.2 Cooperation Gain Comparison

An alternative way to analyze the simulated results to determine the performance improvement through cooperation compared to SUSTC is to use the cooperation gain defined in [35] as

$$G_f = \frac{P_f^{No-Coop}}{P_f^{Coop}} = \frac{P_f^{QS}}{(1-P_f^{in})P_f^{BF} + P_f^{in}P_f^{QS}} = \frac{1}{(1-P_f^{in})\Theta_f + P_f^{in}} \tag{4.1}$$

where $P_f^{No-Coop} = P_f^{QS}$ and $\Theta_f = \frac{P_f^{BF}}{P_f^{QS}}$ is the ratio of cooperative blocking fading FER to quasi-static FER for the users. When $G_f > 1$, the users benefit from cooperation with a lower FER.

Most of the previous sections focus on the extreme cases where the users either perfectly decode the partner's information ($P_f^{in} = 0$) or fail to decode the partner's information ($P_f^{in} = 1$). In the following sections, the FER performance of SUSTC and CSTC for different values of (ρ_s ρ_e) and inter-user channel qualities are presented. Cooperation gains are then computed from the simulation results in order to determine the benefits of CSTC over SUSTC under different channel conditions.

4.2.1 Perfect Channel Estimation ($\rho_e = 1$)

The FER curves and cooperation gains for SUSTC and CSTC with spatially correlated fading, perfect channel estimation, and different P_f^{in} values are presented in this section.

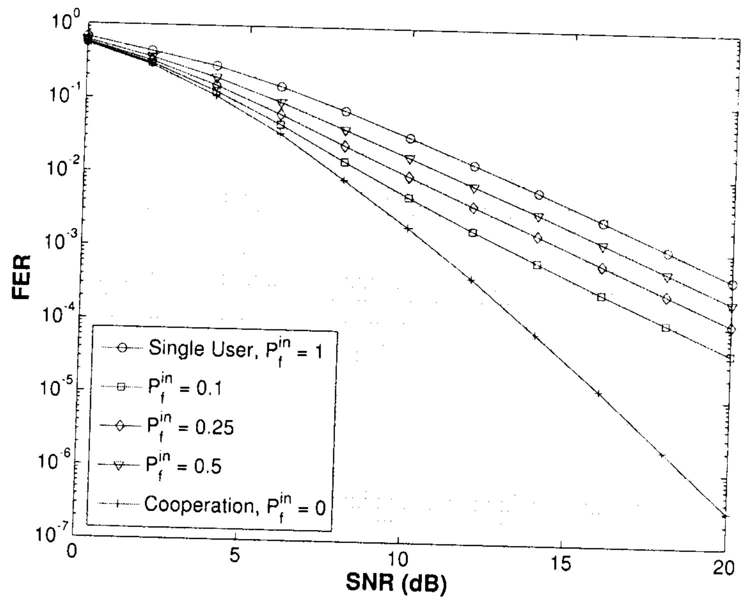

Figure 4.8: Simulation Results for Cooperative Space Time Coding with $\rho_s = 0$, $\rho_e = 1$, and $P_f^{in} =$ 0.1, 0.25, 0.5

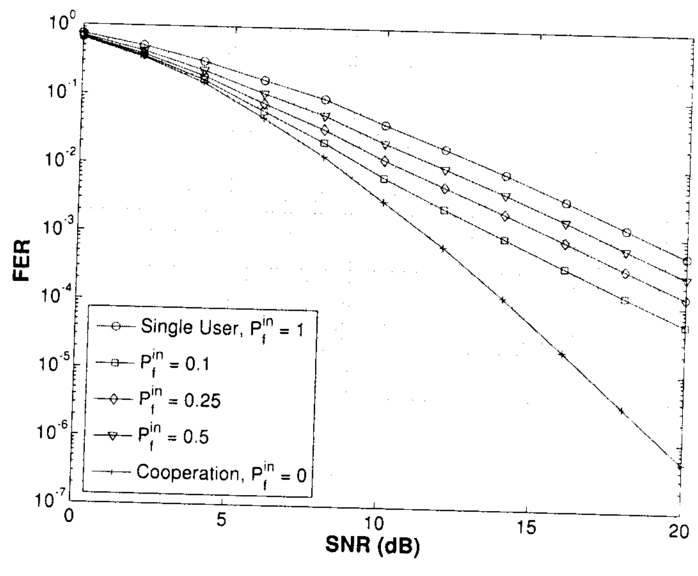

Figure 4.9: Simulation Results for Cooperative Space Time Coding with $\rho_s = 0.5$, $\rho_e = 1$, and $P_f^{in} =$ 0.1, 0.25, 0.5

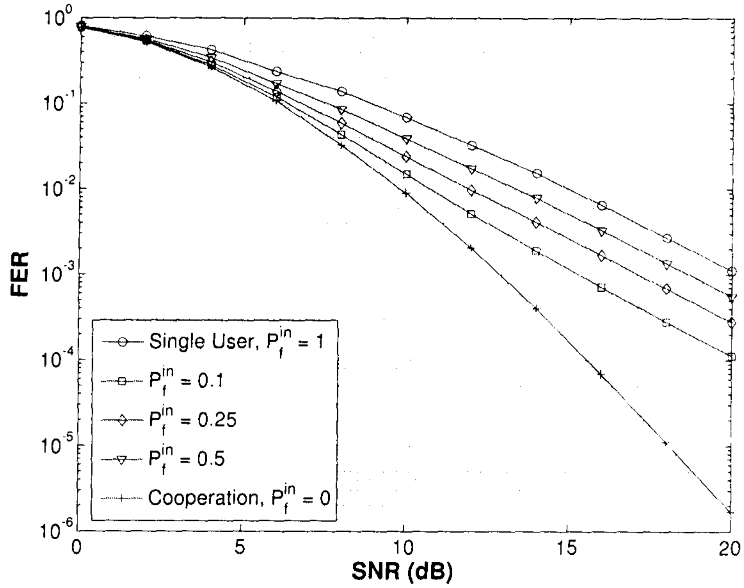

Figure 4.10: Simulation Results for Cooperative Space Time Coding with $\rho_s = 0.8$, $\rho_r = 1$, and $P_f^{in} = 0.1, 0.25, 0.5$

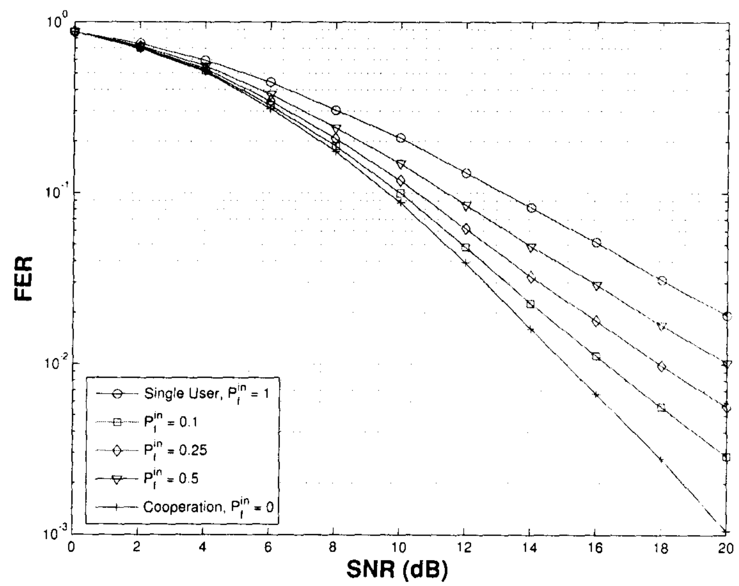

Figure 4.11: Simulation Results for Cooperative Space Time Coding with $\rho_s = 1$, $\rho_r = 1$, and $P_f^{in} = 0.1, 0.25, 0.5$

Table 4.1: Cooperation Gains for $\rho_e = 1$, $P_f^{in} = 0.1$, 0.25, and 0.5

SNR	$\rho_s = 0$	$\rho_s = 0.5$	$\rho_s = 0.8$	$\rho_s = 1$
$P_f^{in} = 0.1$				
8	4.9098	4.3508	3.2021	1.6220
12	7.9517	7.5144	6.3890	2.7062
16	9.6759	9.5377	9.1398	4.6209
20	9.9694	9.9575	9.9113	6.7045
$P_f^{in} = 0.25$				
8	2.9727	2.7917	2.3424	1.4696
12	3.6837	3.6028	3.3659	1.6423
16	3.9558	3.9364	3.8783	2.8818
20	3.9959	3.9943	3.9881	3.4369
$P_f^{in} = 0.5$				
8	1.7934	1.7478	1.6183	1.2707
12	1.9444	1.9291	1.8818	1.3527
16	1.9926	1.9893	1.9793	1.7709
20	1.9993	1.9991	1.9980	1.8964

Figures 4.8 to 4.11 show the FER curves of the single user performance and the two-user cooperation systems with different ρ_s values, perfect channel estimation, and different inter-user channel qualities. From the FER curves, Table 4.1 is obtained. From Table 4.1, we observe that with perfect channel estimation ($\rho_e = 1$), G_f decreases with increasing ρ_s when $P_f^{in} = 0.1$, 0.25, and 0.5. For example, as ρ_s increases from 0 to 0.8 at SNR equals to 20 dB and $P_f^{in} = 0.1$, G_f decreases from 9.9694 to 9.9113. This is expected because as the channel gains get more correlated, the benefit from the diversity decreases. Even when ρ_s increases to 1, where the two channel gains are fully correlated or when the inter-user channel quality gets very poor ($P_f^{in} = 0.5$), the users still benefit from cooperation as G_f does not fall below 1. For example, as P_f^{in} increases from 0.1 to 0.5, G_f decreases from 9.5377 to 1.9893 at $\rho_s = 0.5$ and SNR equals to 16 dB.

4.2.2 Imperfect Channel Estimation ($\rho_e = 0.99$ and 0.9)

The FER curves and cooperation gains for SUSTC and CSTC with spatially correlated fading, imperfect channel estimation, and different P_f^{in} values are presented in this section.

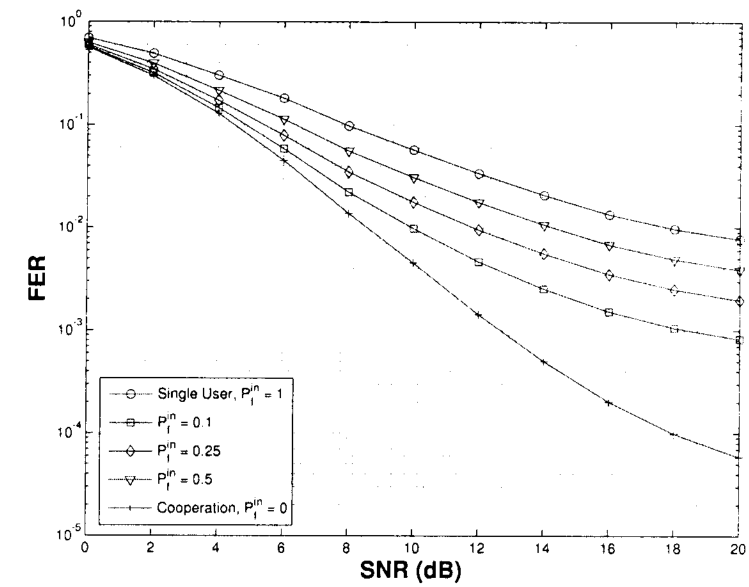

Figure 4.12: Simulation Results for Cooperative Space Time Coding with $\rho_s = 0$, $\rho_c = 0.99$, and P_f^{in} = 0.1, 0.25, 0.5

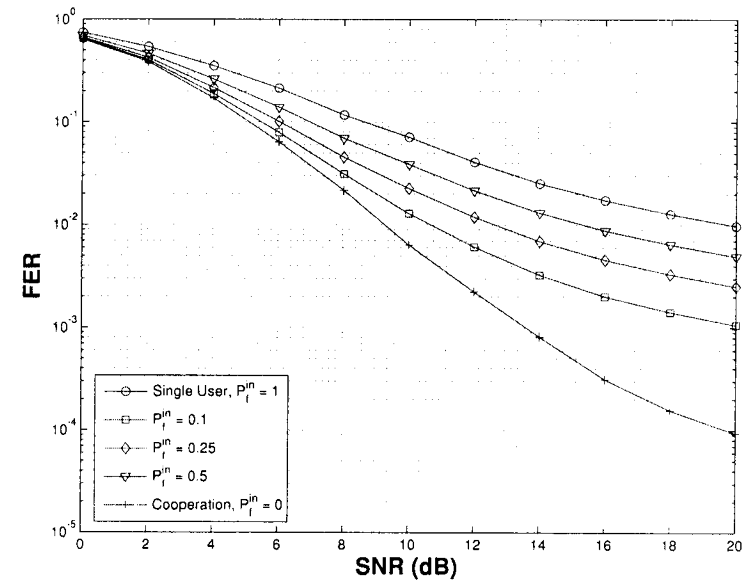

Figure 4.13: Simulation Results for Cooperative Space Time Coding with $\rho_s = 0.5$, $\rho_c = 0.99$, and P_f^{in} = 0.1, 0.25, 0.5

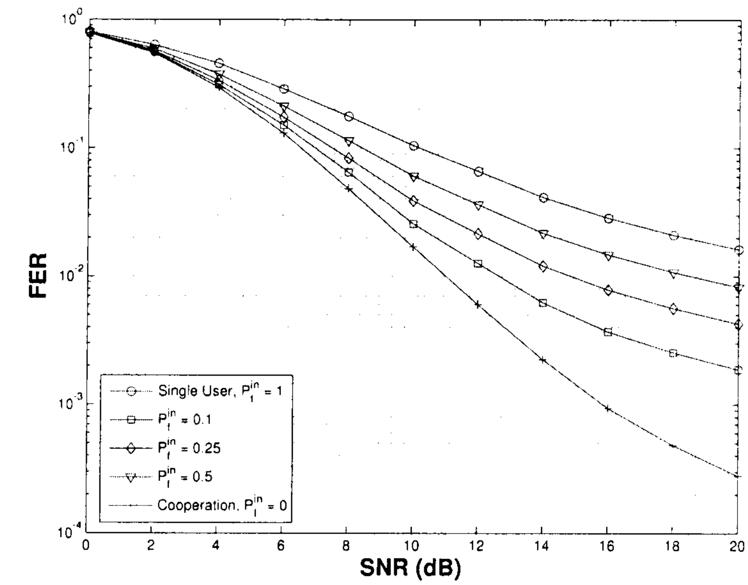

Figure 4.14: Simulation Results for Cooperative Space Time Coding with $\rho_s = 0.8$, $\rho_e = 0.99$, and P_f^{in} = 0.1, 0.25, 0.5

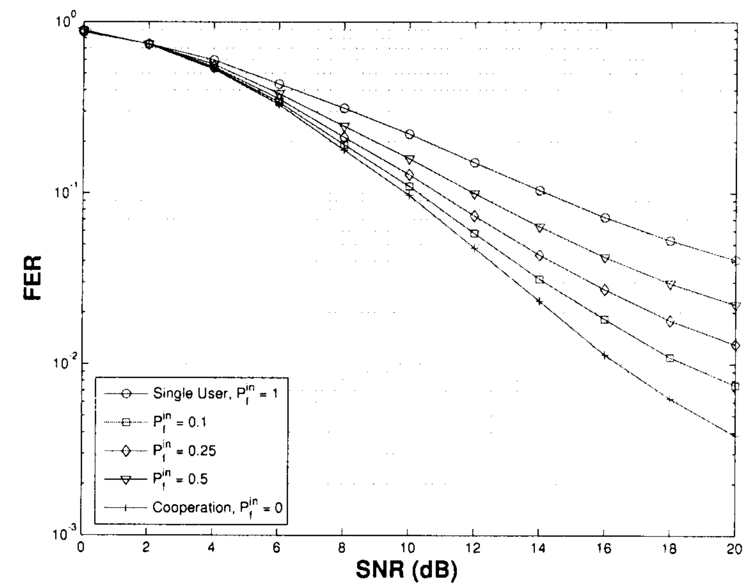

Figure 4.15: Simulation Results for Cooperative Space Time Coding with $\rho_s = 1$, $\rho_e = 0.99$, and P_f^{in} = 0.1, 0.25, 0.5

Table 4.2: Cooperation Gains for $\rho_e = 0.99$, $P_f^{in} = 0.1, 0.25$, and 0.5

SNR	$\rho_s = 0$	$\rho_s = 0.5$	$\rho_s = 0.8$	$\rho_s = 1$
$P_f^{in} = 0.1$				
8	4.4187	3.7508	2.7234	1.6328
12	7.2425	6.6980	5.2073	2.5997
16	8.8034	8.5972	7.7203	3.9387
20	9.3620	9.2076	8.6607	5.4077
$P_f^{in} = 0.25$				
8	2.8149	2.5717	2.1157	1.4770
12	3.5495	3.4355	3.0609	2.0525
16	3.8266	3.7937	3.6416	2.6438
20	3.9112	3.8885	3.8039	3.1175
$P_f^{in} = 0.5$				
8	1.7539	1.6876	1.5422	1.2744
12	1.9188	1.8961	1.8144	1.5194
16	1.9702	1.9644	1.9365	1.7080
20	1.9850	1.9811	1.9662	1.8276

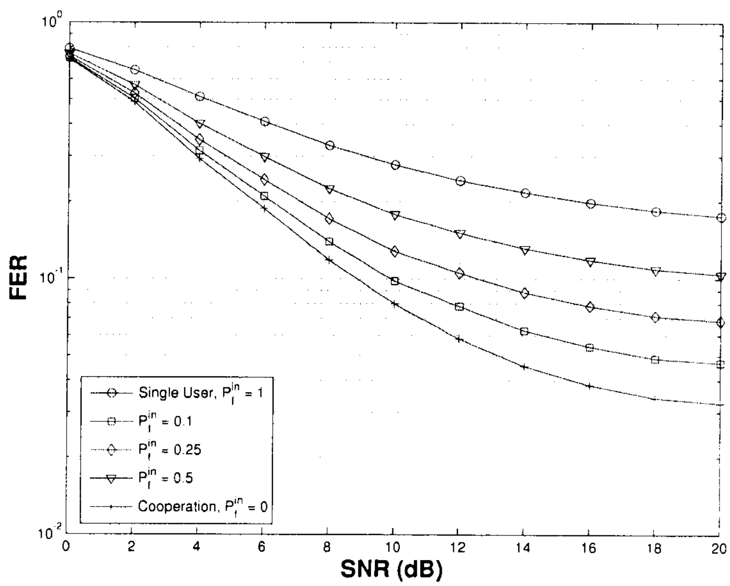

Figure 4.16: Simulation Results for Cooperative Space Time Coding with $\rho_s = 0$, $\rho_e = 0.9$, and $P_f^{in} =$ 0.1, 0.25, 0.5

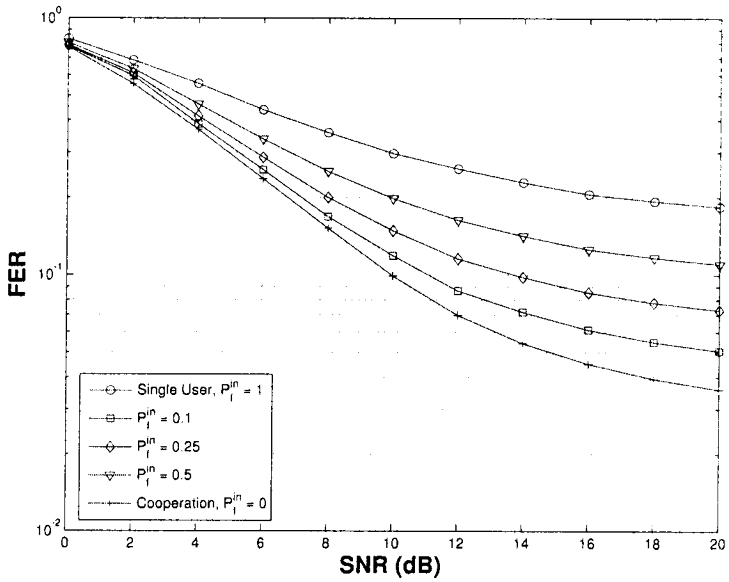

Figure 4.17: Simulation Results for Cooperative Space Time Coding with $\rho_s = 0.5$, $\rho_e = 0.9$, and P_f^{in} = 0.1, 0.25, 0.5

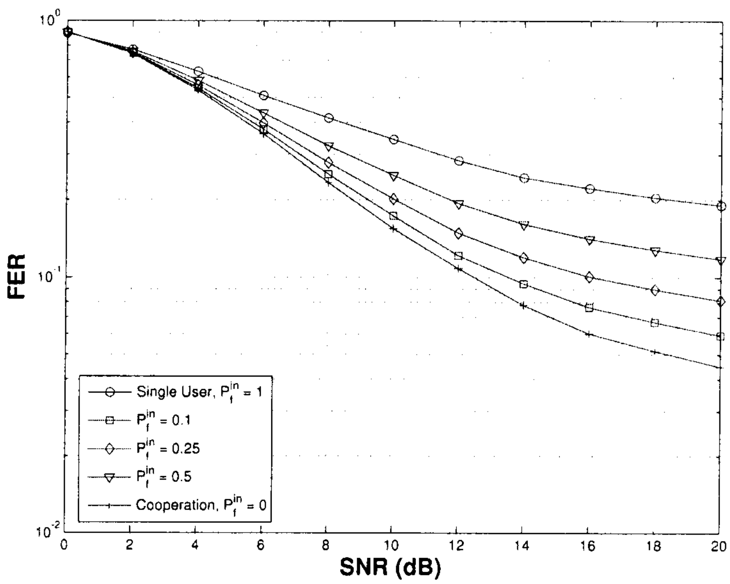

Figure 4.18: Simulation Results for Cooperative Space Time Coding with $\rho_s = 0.8$, $\rho_e = 0.9$, and P_f^{in} = 0.1, 0.25, 0.5

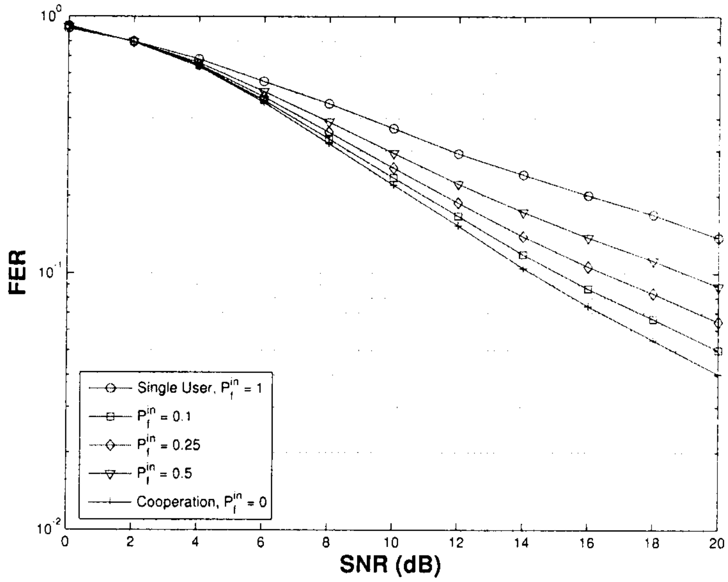

Figure 4.19: Simulation Results for Cooperative Space Time Coding with $\rho_s = 1$, $\rho_e = 0.9$, and $P_f^{in} = 0.1, 0.25, 0.5$

Table 4.3: Cooperation Gains for $\rho_e = 0.9$, $P_f^{in} = 0.1$, 0.25, and 0.5

SNR	$\rho_s = 0$	$\rho_s = 0.5$	$\rho_s = 0.8$	$\rho_s = 1$
$P_f^{in} = 0.1$				
8	2.3722	2.0732	1.6544	1.3719
12	3.1596	2.9190	2.2551	1.7470
16	3.6453	3.3647	2.8995	2.3077
20	3.7468	3.6360	3.2107	2.7396
$P_f^{in} = 0.25$				
8	1.9306	1.7587	1.4917	1.2919
12	2.3234	2.2117	1.8650	1.5536
16	2.5299	2.4135	2.2023	1.8947
20	2.5702	2.5262	2.3462	2.1238
$P_f^{in} = 0.5$				
8	1.4735	1.4037	1.2816	1.1773
12	1.6122	1.5754	1.4476	1.3116
16	1.6755	1.6405	1.5722	1.4595
20	1.6871	1.6744	1.6195	1.5450

Figures 4.12 to 4.19 show the FER curves of the single user performance and the two-user cooperation systems with different ρ_s values, imperfect channel estimation ($\rho_e = 0.99$ and 0.9), and different inter-user channel qualities ($P_f^{in} = 0.1$, 0.25, and 0.5). From the FER curves, Tables 4.2 and 4.3 can be obtained. From Tables 4.2 and 4.3, we observe that even with imperfect channel estimation ($\rho_e = 0.9$ and 0.99), the users still benefit from cooperation as G_f is always greater than 1. It is also observed that G_f decreases with increasing ρ_s and P_f^{in}. For example, as ρ_s increases from 0.5 to 0.8 at SNR equals to 20 dB, $P_f^{in} = 0.1$, and $\rho_e = 0.99$, G_f decreases from 9.2076 to 8.6607. This is expected because as the channels get more correlated, the benefit from the diversity decreases even when the channel estimation is not perfect. Similar to the case where the channel estimation is perfect as discussed in the previous section, the users still benefit from cooperation even when ρ_s increases to 1 and when the inter-user channel quality becomes poor ($P_f^{in} = 0.5$).

By comparing Tables 4.1, 4.2, and 4.3, we observe that

- G_f decreases with increasing P_f^{in}.
- G_f decreases with increasing ρ_s.
- G_f decreases with decreasing ρ_e.

The reason that causes G_f to decrease with decreasing ρ_e is not as clear as the reasons that cause G_f to decrease with increasing P_f^{in} and ρ_s because the statistics of the estimated errors are the same for both quasi-static and block fading channels. As ρ_e decreases from 1 to 0.99 with ρ_s, P_f^{in} and SNR equal to 0.5, 0.1, and 20dB, G_f decreases from 9.9575 to 9.2076. As ρ_e decreases to 0.9, G_f decreases to 3.6360. Recall from (4.1) that $\Theta_f = \frac{P_f^{BF}}{P_f^{QS}}$. As ρ_e decreases from 1 to 0.99 and to 0.9, P_f^{BF} decreases faster than P_f^{QS}, thus causing G_f to decrease with decreasing ρ_e. From the Tables and discussions above, it can be concluded that even though the channel estimation is not perfect ($\rho_e = 0.99$ and 0.9), the users still benefit from cooperation.

It is assumed that the channel estimation correlation coefficient ρ_e is fixed in the analysis discussed in this Chapter. However, the changes in SNR will affect the accuracy of the channel estimation model. The influence of SNR to ρ_e varies with different channel estimation models. For example, as in [11], we can define ρ_e as $\rho_e = \frac{1}{\sqrt{1+\frac{1}{SNR}}}$ for the channel estimation model described in this thesis.

Chapter 5

STC with Impulsive Noise

In this chapter, the FER performance of SUSTC with spatially correlated fading, channel estimation error, and impulsive noise is investigated. A decision metric is obtained in Section 5.1 and FER simulation results are presented in Section 5.2.

5.1 System Model with Mixture Gaussian Noise

The system model is the same as that in Chapter 3 except the pdf's of the imaginary and real parts of the noise r.v. N_t are statistically dependent Gaussian mixture distributed as defined in (2.4).

With the mean and variance of the received signal at time t given by (3.29) and (3.30), the pdf of R_t given the estimated channel gains is

$$\begin{aligned} P(r_t|c_{t,i}^k, H_{j,i} = h_{j,i}, i, j = 1, 2) &= (1-\epsilon)\frac{1}{\sqrt{2\pi\sigma_X^2}} \exp\left[-\frac{|r_t - \sqrt{E_s}\sum_{i=1}^{2} c_{t,i}^k m_{j,i}|^2}{2\sigma_X^2}\right] \\ &+ \epsilon\frac{1}{\sqrt{2\pi\sigma_Y^2}} \exp\left[-\frac{|r_t - \sqrt{E_s}\sum_{i=1}^{2} c_{t,i}^k m_{j,i}|^2}{2\sigma_Y^2}\right] \end{aligned} \quad (5.1)$$

with

$$\sigma_X^2 = E_s\frac{(1-\rho_e^2)(1-\rho_s^2\rho_e^2)}{1-\rho_s^2\rho_e^4} + 2E_s c_{t,1}^k c_{t,2}^k \rho_d \sigma_D^2 + \sigma_\eta^2 \quad (5.2)$$

and

$$\sigma_Y^2 = E_s \frac{(1-\rho_e^2)(1-\rho_s^2\rho_e^2)}{1-\rho_s^2\rho_e^4} + 2E_s c_{t,1}^k c_{t,2}^k \rho_d \sigma_D^2 + \sigma_I^2 \tag{5.3}$$

where j denotes the user, $c_{t,i}^k$ denotes the coded bit to be transmitted by antenna i in segment k at time t, and $m_{j,i}$ (i,j = 1,2) is given in (3.19) and (3.20) for the respective user. The expression in the numerator of the exponential for the first segment $(t = 1, ..., L)$ is

$$|r_t - \sqrt{E_s}\sum_{i=1}^{2} c_{t,i}^1 m_{1,i}|^2 \tag{5.4}$$

When cooperation takes place, the expression in the numerator of the exponential for the second segment $(t = L+1, ..., 2L)$ is

$$|r_t - \sqrt{E_s}\sum_{i=1}^{2} c_{t,i}^2 m_{2,i}|^2. \tag{5.5}$$

When there is no cooperation, the expression in the numerator of the exponential for the second segment is

$$|r_t - \sqrt{E_s}\sum_{i=1}^{2} c_{t,i}^2 m_{1,i}|^2 \tag{5.6}$$

with $t = L+1, ..., 2L$.

With the assumption that the components of the received vector given the estimated channel gains are independent, the mixture Gaussian decision metric (MGDM) for SUSTC can be obtained by taking the logarithm of (5.1) to minimizes the quantity

$$-\sum_{k=1}^{2}\sum_{t=1}^{L} \log P(r_t|c_{t,1}^k, c_{t,2}^k, H_{1,1} = h_{1,1}, H_{1,2} = h_{1,2}). \tag{5.7}$$

Similarly, the MGDM for CSTC can be expressed as

$$-\sum_{k=1}^{2}\sum_{t=1}^{L} \log P(r_t|c_{t,1}^k, c_{t,2}^k, H_{k,1} = h_{k,1}, H_{k,2} = h_{k,2}). \tag{5.8}$$

5.2 Numerical Results

Simulations were performed with $\rho_e = 1$ and 0.99 and highly impulsive noise ($\frac{\sigma_I^2}{\sigma_n^2} = 500$, $\epsilon = 0.05$). The convolutional codes [5 7] and [5 7] were used for User 1 and User 2 respectively.

5.2.1 Perfect Channel Estimation ($\rho_e = 1$)

When $\rho_e = 1$, (5.1) reduces to

$$P(r_t|G_{j,i} = g_{j,i}, i, j = 1, 2) = (1-\epsilon)\frac{1}{\sqrt{2\pi\sigma_\eta^2}} \exp\left[-\frac{|r_t - \sqrt{E_s}\sum_{i=1}^{2} c_{t,i}^k g_{j,i}|^2}{2\sigma_\eta^2}\right] + \epsilon\frac{1}{\sqrt{2\pi\sigma_I^2}} \exp\left[-\frac{|r_t - \sqrt{E_s}\sum_{i=1}^{2} c_{t,i}^k g_{j,i}|^2}{2\sigma_I^2}\right]. \tag{5.9}$$

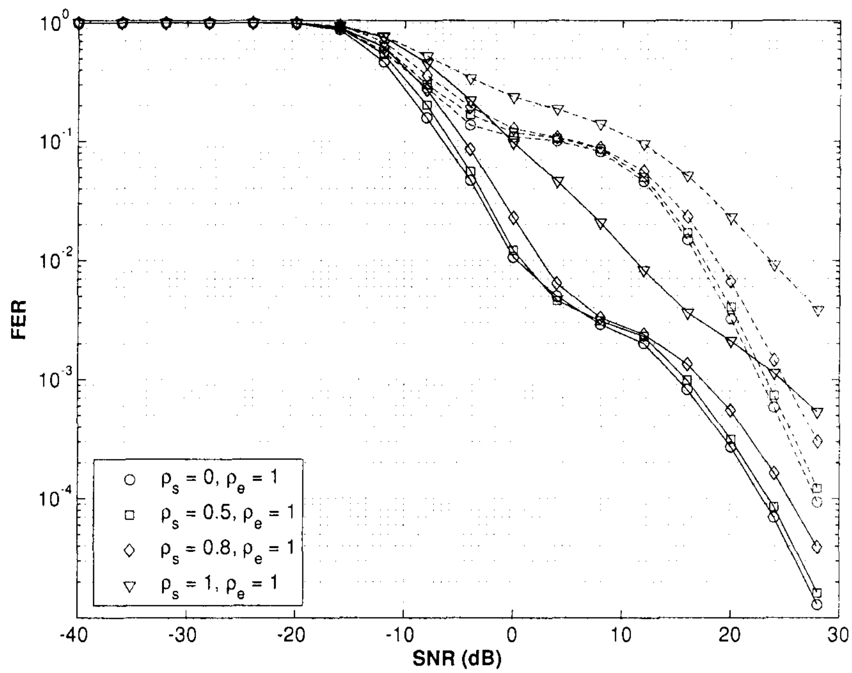

Figure 5.1: SUSTC with $\rho_e = 1$, different ρ_s values, and mixture gaussian noise with $\epsilon = 0.05$ and $\frac{\sigma_I^2}{\sigma_\eta^2} = 500$ (solid: Mixture Gaussian Decision Metric; dashed: Gaussian Decision Metric)

The FER of SUSTC as a function of SNR for spatially correlated fading, perfect channel estimation ($\rho_e = 1$), and mixture Gaussian noise is plotted in Figure 5.1 with $\epsilon = 0.05$ and $\frac{\sigma_I^2}{\sigma_\eta^2} = 500$. The solid line shows the performance when the proposed MGDM in (5.7) is used whereas the dashed line shows the performance with the Gaussian decision metric (GDM) in (3.38). It can be seen that the MGDM provides a better performance than the GDM. This is expected since the MGDM in (5.7) is optimal when there is no channel estimation error. With channel estimation error, (5.7) is no longer optimal because the components of the received vector are no longer independent. One disadvantage of the MGDM is that the impulsive noise parameters, i.e. ϵ and $\frac{\sigma_I^2}{\sigma_\eta^2}$, are required at the receiver.

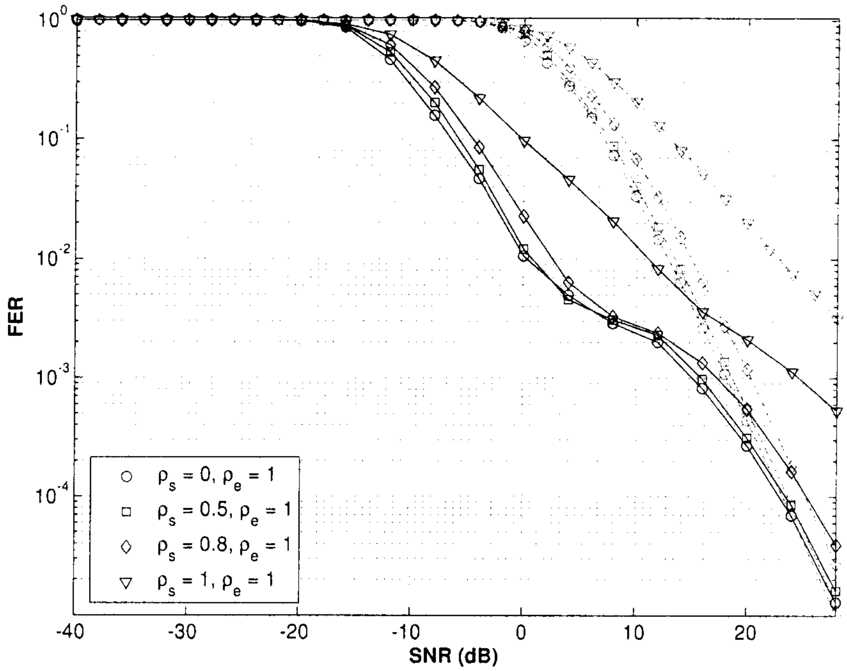

Figure 5.2: SUSTC with $\rho_e = 1$, different ρ_s values, and mixture Gaussian noise with $\epsilon = 0.05$ and $\frac{\sigma_I^2}{\sigma_\eta^2} = 500$ (dashed: Gaussian Noise with GDM; solid: Mixture Gaussian Noise with MGDM)

The FER curves of SUSTC as a function of SNR with Gaussian noise and Mixture Gaussian noise are shown in Figure 5.2. It can be seen that the FER with Mixture Gaussian noise and MGDMof (5.7) (solid lines) is lower than with Gaussian noise and GDM of (3.38) at lower SNR values. As the SNR increases beyond 24 dB, the $\rho_s = 0$ FER curve with Gaussian noise crosses that with mixture Gaussian noise. This is because of the heavier tail of the mixture Gaussian pdf as shown in Figure 2.2. The performance bounds for optimum reception under class-A impulsive noise was discussed in [20]. It is observed in [20] that as SNR increases, the slopes of the curves with Gaussian and class-A impulsive noises are the same. From Figure 5.2, it can be observed that the asymptotic slopes of the curves are similar for ρ_s = 0, 0.5, 0.8. It is expected that the asymptotic slopes of the FER curves with Gaussian and Mixture Gaussian noises will be the same. The FER curves at higher SNR values were not simulated due to the excessive times needed.

5.2.2 Imperfect Channel Estimation ($\rho_e = 0.99$)

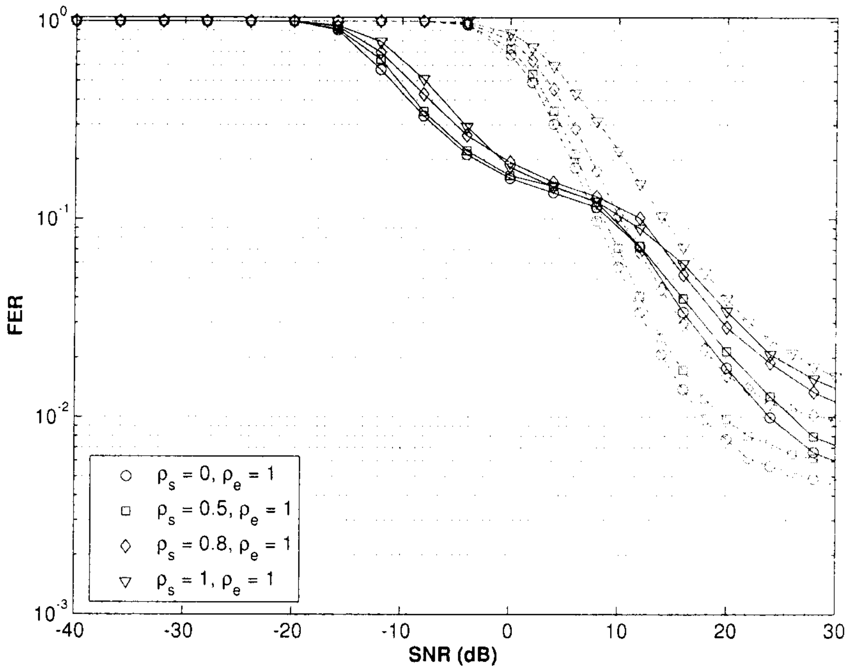

Figure 5.3: SUSTC with $\rho_e = 0.99$, different ρ_s values, and mixture Gaussian noise with $\epsilon = 0.05$ and $\frac{\sigma_I^2}{\sigma_\eta^2} = 500$ (solid: Mixture Gaussian Noise with MGDM; dashed: Gaussian Noise with GDM)

The FER of SUSTC as a function of SNR for spatially correlated fading, imperfect channel estimation ($\rho_e = 0.99$), and Gaussian and mixture Gaussian ($\epsilon = 0.05$ and $\frac{\sigma_I^2}{\sigma_\eta^2} = 500$) noises is plotted in Figure 5.3. Similar to the case with perfect channel estimation, it is observed that SUSTC shows better performance with mixture Gaussian noise than with Gaussian noise at low SNR. At high SNR, the FER with Gaussian noise is lower than that with mixture Gaussian noise.

The performance of Cooperative Space Time Coding (CSTC) was not simulated in this chapter due to the time constraints. Since the diversity order of a system depends on the number of independent fading paths, it is expected that the performance of CSTC will be qualitatively similar to that of SUSTC except that the slopes of the CSTC curves will be steeper.

Chapter 6

Conclusion

6.1 Main Thesis Contributions

A performance study of cooperative space time coding with spatially correlated fading and imperfect channel estimation in Gaussian as well as impulsive noise was presented. The main contributions of the thesis are listed below.

• Closed form expressions for the pairwise error probability conditioned on the estimated channel gains with spatially correlated fading and imperfect channel estimation are derived for 1) single user space time coding (SUSTC) with quasi-static fading channels and 2) cooperative space time coding (CSTC) with block fading channels. An expurgated bound on the FER for both cases is then obtained using the limiting before average technique in [33] and assuming the components of the received vector are independent given the estimated channel gains.

• Simulation results for a constraint length 3 convolutional code were compared with the analytical bounds. The results show that even though the bound is not very tight, it is able to capture the performance degradation as ρ_s increases perfectly when $\rho_e = 1$. As ρ_e decreases, the performance degradation of the simulation results and the bounds are different because of the channel estimation error.

• The cooperation gains show that the users always benefit from cooperation even in the case where the channel gains within each user are strongly correlated ($\rho_s \approx 1$) and when the channel estimations are very poor ($\rho_e \approx 0.9$) because CSTC with block fading channels have a lower FER compared to SUSTC with quasi-static fading channels.

• A detailed discussion on the dependency among the components of the received vector for a system with space time trellis codes was presented. The discussion confirms with the observation in [30] that the components of the received vector are not independent and shows that the introduction of the channel estimation error is the reason for this dependency.

• A decision metric for CSTC with spatially correlated fading, imperfect channel estimation, and mixture Gaussian noise is derived. Simulation results show that, by using the proposed mixture Gaussian decision metric for CSTC with mixture Gaussian noise, the FER performance of CSTC with mixture Gaussian noise is better than that of CSTC with Gaussian noise at low SNR. At high SNR, CSTC with Gaussian noise outperforms CSTC with mixture Gaussian noise because of the heavy tail of the mixture Gaussian noise.

6.2 Topics for Further Studies

• Extensions of the thesis work to other modulation, channel fading, channel estimation, or different impulsive noise models can be made.

• More investigations can be carried out on CSTC with spatially correlated fading and poor channel estimation ($\rho_e \leq 0.9$) to provide a more complete picture of the FER performance.

Appendix A

Dependencies among the components of the received vector

In [31], the performance of space-time codes with two transmit and one receive antennas and their design criteria in the presence of channel estimation errors was examined. In the performance analysis, the received signal at time t is denoted as

$$r_t = \sqrt{E_s} \sum_{i=1}^{2} g_i c_{t,i} + n_t \tag{A.1}$$

where the channel gains, g_1 and g_2, and noise component at time t are modeled as independent samples of a zero mean complex Gaussian r.v.'s with variance σ_G^2 and $\frac{N_0}{2}$ respectively. If a codeword

$$\mathbf{c} = c_{1,1}c_{1,2}\ c_{2,1}c_{2,2}...c_{L,1}c_{L,2} \tag{A.2}$$

is sent, the corresponding received vector is

$$\mathbf{r} = r_1\ r_2\ r_3...r_L \tag{A.3}$$

where L denotes the frame length. At the receiver, ML decoding is used. The codeword

$$\mathbf{e} = e_{1,1}e_{1,2}\ e_{2,1}e_{2,2}...e_{L,1}e_{L,2} \tag{A.4}$$

is chosen for which $\Pr(\mathbf{r}|\mathbf{e}, \mathbf{H} = \mathbf{h})$ is maximized where $\mathbf{H} = [H_1 H_2]$ and $\mathbf{h} = [h_1 h_2]$.

It is assumed in [31] that the components of the received vector are independent given the estimated channel gains. Then ML decoding simplifies to choosing the codeword which minimizes

$$\sum_{t=1}^{L} -\log \Pr(\mathbf{r}|\mathbf{e}, \mathbf{H} = \mathbf{h}) \tag{A.5}$$

We look at the covariance between the received signals at a two time instance to explain the dependencies among the components of the received vector. The covariance between two complex r.v.'s X and Y is

$$Cov\{XY\} = E\{XY^*\} - E\{X\}E\{Y^*\} \tag{A.6}$$

Let X = R_1 and Y = R_2. We now compute $E[R_1 R_2^*|\mathbf{H}]$ and $E[R_1|\mathbf{H}]E[R_2^*|\mathbf{H}]$ for Alamouti coding and the model in Chapter 3 for quasi-static fading to determine if the components of the received vectors are independent given the estimated channel gains.

For Alamouti coding with quasi static fading, we have

$$\begin{aligned} r_1 &= g_1 s_1 + g_2 s_2 + n_1 \\ r_2 &= -g_1 s_2^* + g_2 s_1^* + n_2 \end{aligned} \tag{A.7}$$

where s_1 and s_2 are the transmitted signals and the covariance of R_1 and R_2 given the estimated channel gains, H_1 and H_2, can be computed as

$$\begin{aligned} E[R_1 R_2^*|\mathbf{H}] &= E[((G_1|\mathbf{H})s_1 + (G_2|\mathbf{H})s_2 + N_1)((-G_1|\mathbf{H})s_2 + (G_2|\mathbf{H})s_1 + N_2)^*] \\ &= E[m_1 m_2 s_1^2 - m_1 m_2 s_2^2 + s_1 s_2 m_2^2 - s_1 s_2 m_1^2 + \rho_d \sigma_D^2 s_1^2 - \rho_d \sigma_D^2 s_2^2] \end{aligned} \tag{A.8}$$

$$\begin{aligned} E[R_1|\mathbf{H}]E[R_2^*|\mathbf{H}] &= E[(G_1|\mathbf{H})s_1 + (G_2|\mathbf{H})s_2 + N_1]E[((-G_1|\mathbf{H})s_2 + (G_2|\mathbf{H})s_1 + N_2)^*] \\ &= E[m_1 m_2 s_1^2 - m_1 m_2 s_2^2 + s_1 s_2 m_2^2 - s_1 s_2 m_1^2] \end{aligned} \tag{A.9}$$

with m_1, m_2, ρ_d, and σ_D^2 given in Chapter 3.

With $E\{s_i^2\} = 1$ for the case of BPSK modulation, we have

$$E[R_1 R_2^*|\mathbf{H}] - E[R_1|\mathbf{H}]E[R_2^*|\mathbf{H}] = 0. \tag{A.10}$$

It is shown in Chapter 3 that $\sigma^2_{G_1|\mathbf{H}} = \sigma^2_{G_2|\mathbf{H}}$. With the assumption that the real and imaginary parts of the complex r.v.'s are independent, it can be shown that $E[R_1R_2^*|\mathbf{H}]$ $= E[R_1^*R_2|\mathbf{H}]$. Thus, the covariance of R_1 and R_2 given the estimated channels shows that the components of the received vector with Alamouti coding and quasi static fading are independent.

For the single user space time model with quasi-static fading discussed in Chapter 3, we have

$$\begin{aligned} r_t &= g_1 c_{t,1} + g_2 c_{t,2} + n_t \\ &= m_1 c_{t,1} + m_2 c_{t,2} + d_1 c_{t,1} + d_2 c_{t,2} + n_t \end{aligned} \tag{A.11}$$

where m_1, m_2, d_1, and d_2 given in Chapter 3. ($\sqrt{E_s}$ is dropped from the equation to simplify the derivation as it does not affect the result.)

The covariance of R_1 and R_2 given $\mathbf{H}$ is

$$\begin{aligned} E[R_1R_2^*|\mathbf{H}] &= E[(c_{1,1}(G_1|\mathbf{H}) + c_{1,2}(G_2|\mathbf{H}) + N_1)(c_{2,1}(G_1|\mathbf{H}) + c_{2,2}(G_2|\mathbf{H}) + N_2)^*] \\ &= E[c_{1,1}c_{2,1}m_1^2 + c_{1,2}c_{2,2}m_2^2 + c_{1,1}c_{2,2}m_1m_2 + c_{1,2}c_{2,1}m_1m_2] \\ &+ E[c_{1,1}c_{2,1} + c_{1,2}c_{2,2} + c_{1,1}c_{2,2}\rho_d + c_{1,2}c_{2,1}\rho_d]\sigma_D^2 \end{aligned} \tag{A.12}$$

$$\begin{aligned} E[R_1|\mathbf{H}]E[R_2^*|\mathbf{H}] &= E[(c_{1,1}(G_1|\mathbf{H}) + c_{1,2}(G_2|\mathbf{H}) + N_1)]E[(c_{2,1}(G_1|\mathbf{H}) + c_{2,2}(G_2|\mathbf{H}) + N_2)^*] \\ &= E[c_{1,1}c_{2,1}m_1^2 + c_{1,2}c_{2,2}m_2^2 + c_{1,1}c_{2,2}m_1m_2 + c_{1,2}c_{2,1}m_1m_2] \end{aligned} \tag{A.13}$$

$$\begin{aligned} E[R_1R_2^*|\mathbf{H}] - E[R_1|\mathbf{H}]E[R_2^*|\mathbf{H}] &= E[c_{1,1}c_{2,1}]\sigma_D^2 + E[c_{1,2}c_{2,2}]\sigma_D^2 \\ &+ E[c_{1,1}c_{2,2}]\rho_d\sigma_D^2 + E[c_{1,2}c_{2,1}]\rho_d\sigma_D^2 \end{aligned} \tag{A.14}$$

For the single user space time model, we still have $E[R_1R_2^*|\mathbf{H}] = E[R_1^*R_2|\mathbf{H}]$, $\sigma^2_{G_1|\mathbf{H}} = \sigma^2_{G_2|\mathbf{H}}$, and $E[c_{i,j}]^2 = 1$ (i,j = 1,2), but the covariance between R_1 and R_2 are no longer zero. This shows that the components of the received vector are not independent given the estimated channel gains.

For the case with independent channel gains and perfect channel estimation as in [4], the covariance of R_1 and R_2 given G_1 and G_2 can be easily shown to be zero. Following the above discussions, we conclude that the introduction of the channel estimation error conditioned on the estimated channel gains causes the components of the received vector to depend on each other. This confirms with the result in [30] but provides a more detail explanation on the dependencies among the components of the received vector.

Appendix B

Extended Trellis

From (3.52), the distance term $d^2(c,e)$ depends on the number of transmit antennas. Following a similar derivation as that in [34], the $d^2(c,e)$ term for a block fading channel is

$$\begin{aligned} d^2_{BF}(c,e) &= \sum_{b=1}^{2}\sum_{t=1}^{L}|\sum_{i=1}^{2} m_{b,i}(c^b_{t,i} - e^b_{t,i})|^2 \\ &= \sum_{b=1}^{2}|m_{b,1}|^2 A^1_{b,1} + \sum_{b=1}^{2}|m_{b,2}|^2 A^2_{b,2} \\ &+ 2\Re\{\sum_{b=1}^{2}(m_{b,1}m^*_{b,2})B_b\} \end{aligned} \quad \text{(B.1)}$$

where

$$A^1_{b,1} = \sum_{t=1}^{L}|(c^b_{t,1} - e^b_{t,1})|^2 \quad \text{(B.2)}$$

$$A^2_{b,2} = \sum_{t=1}^{L}|(c^b_{t,2} - e^b_{t,2})|^2 \quad \text{(B.3)}$$

$$B_b = \sum_{t=1}^{L}(c^b_{t,1} - e^b_{t,1})(c^b_{t,2} - e^b_{t,2})^* \quad \text{(B.4)}$$

, L denotes the number of bits in each block, and b denotes the block (segment) index.

As in Chapter 3, if the partner fails to decode the user's information, the user continues to transmit the remaining parts of the coded bits in the second time segment. Thus.

quasi-static channel can be viewed as a block fading channel except the channel gains are the same in both blocks (segments) and the $d^2(c, e)$ term can be expressed as

$$\begin{aligned} d^2_{QS}(c, e) &= \sum_{t=1}^{L} |\sum_{i=1}^{2} m_{1,i}(c_{t,i} - e_{t,i})|^2 \\ &= 2|m_{1,1}|^2 A_1^1 + 2|m_{1,2}|^2 A_2^2 \\ &+ 2\Re\{2(m_{1,1}m_{1,2}^*)B\} \end{aligned} \tag{B.5}$$

where

$$A_1^1 = \sum_{t=1}^{L} |(c_{t,1} - e_{t,1})|^2 \tag{B.6}$$

$$A_2^2 = \sum_{t=1}^{L} |(c_{t,2} - e_{t,2})|^2 \tag{B.7}$$

$$B = \sum_{t=1}^{L} (c_{t,1} - e_{t,1})(c_{t,2} - e_{t,2})^* \tag{B.8}$$

In order to find a bound for CSTC system, we need to know the weight enumerating function, or distance spectrum of the space time trellis code [36]. We made use of the technique in [33] where it keeps track of all the real variables A_1^1, A_2^2, B as in (B.2) to (B.4) and (B.6) to (B.8) and claims that the weight enumerating function is the multiplicities of the these real variables over all codeword pairs. Since BPSK modulation is used, B is also a real variable.

In this thesis, convolutional encoding with constraint length 4 and generator polynomial $g = [5\ 7]$ is used for both users. The encoding diagram and the corresponding trellis are shown in Figures B.1 and B.2.

The extended trellis for this code is shown in Figure B.3. To obtain the extended trellis, we start by looking at the 4 state trellis in Figure B.2 and computing the distance between the correct path starting from state i, S_i and the erroneous path starting from state j, S_j where i, j = 0, 1, 2, 3. Thus, the states of the extended trellis are of the form "$S_i^{(c)} S_j^{(e)}$" where the correct path (c) and the erroneous path (e) are in state S_i and S_j

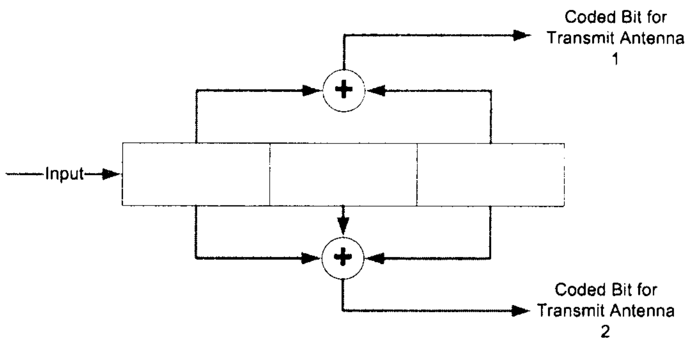

Figure B.1: K = 3, g = [5 7] convolutioanl encoder.

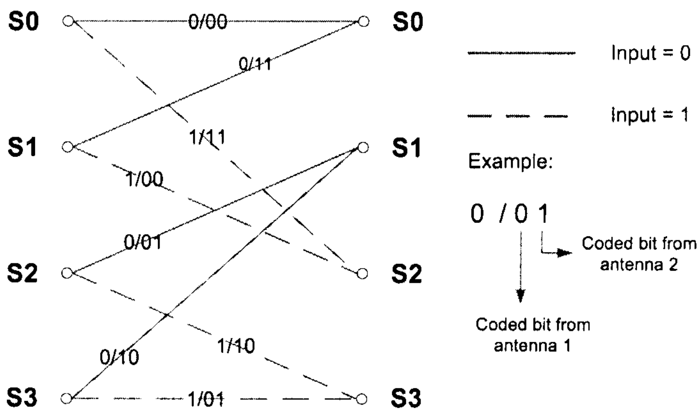

Figure B.2: 4-State Space Time Trellis Code.

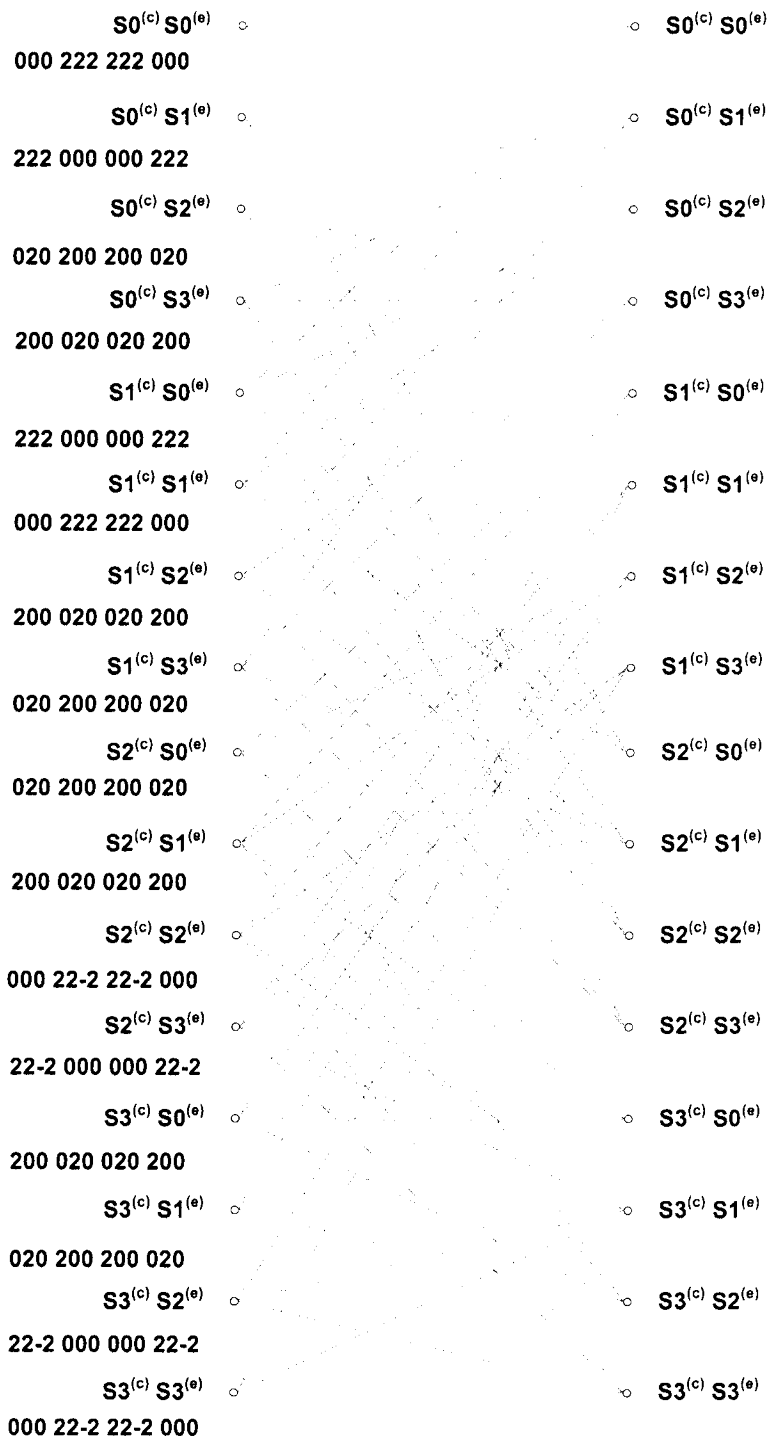

Figure B.3: Extended Trellis for the 4-State Space Time Trellis Code.

of the original 4 state trellis in Figure B.2. The labels on the extended trellis take the form $[X\ Y\ Z]$ and correspond to one state transition of the Euclidean distance between the correct path and the erroneous path for the first transmit antenna, second transmit antenna, and the cross terms between the two antennas. The multiplicities of all state transitions for the entire correct and erroneous sequence are equivalent to (B.2) to (B.4), and (B.6) to (B.8) for block fading and quasi-static channel respectively. For example, let us assume the correct path and the erroneous path start at state zero, which is "$S_0^{(c)}S_0^{(e)}$" in Figure B.3 and the correct path goes to state 2 while the erroneous path stays in state zero, which is "$S_2^{(c)}S_0^{(e)}$" in the next time instance. Then, we have 11 (+1+1 as for BPSK modulation) and 00 (-1-1 as for BPSK modulation) as the outputs on the 4 state trellis for the correct and erroneous paths. Thus, the corresponding Euclidean distance for the two paths for the first transmit antenna, the second transmit antenna, and the cross term for both transmit antennas can then be computed as 222.

The 16 by 16 state transition matrix $\mathbf{S}$ for the extended trellis for the 4 state space time trellis code is then given by (B.9).

$$\mathbf{S}_{\mathbf{1\ to\ 8}} = \begin{bmatrix}
A_1^0A_2^0B^0 & 0 & A_1^2A_2^2B^2 & 0 & 0 & 0 & 0 & 0 \\
A_1^2A_2^2B^2 & 0 & A_1^0A_2^0B^0 & 0 & 0 & 0 & 0 & 0 \\
0 & A_1^0A_2^2B^0 & 0 & A_1^2A_2^0B^0 & 0 & 0 & 0 & 0 \\
0 & A_1^2A_2^0B^0 & 0 & A_1^0A_2^2B^0 & 0 & 0 & 0 & 0 \\
A_1^2A_2^2B^2 & 0 & A_1^0A_2^0B^0 & 0 & 0 & 0 & 0 & 0 \\
A_1^0A_2^0B^0 & 0 & A_1^2A_2^2B^2 & 0 & 0 & 0 & 0 & 0 \\
0 & A_1^2A_2^0B^0 & 0 & A_1^0A_2^2B^0 & 0 & 0 & 0 & 0 \\
0 & A_1^0A_2^2B^0 & 0 & A_1^2A_2^0B^0 & 0 & 0 & 0 & 0 \\
0 & 0 & 0 & 0 & A_1^0A_2^2B^0 & 0 & A_1^2A_2^0B^0 & 0 \\
0 & 0 & 0 & 0 & A_1^2A_2^0B^0 & 0 & A_1^0A_2^2B^0 & 0 \\
0 & 0 & 0 & 0 & 0 & A_1^0A_2^0B^0 & 0 & A_1^2A_2^2B^{-2} \\
0 & 0 & 0 & 0 & 0 & A_1^2A_2^2B^{-2} & 0 & A_1^0A_2^0B^0 \\
0 & 0 & 0 & 0 & A_1^2A_2^0B^0 & 0 & A_1^0A_2^2B^0 & 0 \\
0 & 0 & 0 & 0 & A_1^0A_2^2B^0 & 0 & A_1^2A_2^0B^0 & 0 \\
0 & 0 & 0 & 0 & 0 & A_1^2A_2^2B^{-2} & 0 & A_1^0A_2^0B^0 \\
0 & 0 & 0 & 0 & 0 & A_1^0A_2^0B^0 & 0 & A_1^2A_2^2B^{-2}
\end{bmatrix}$$

$$
\mathbf{S}_{\mathbf{9\ to\ 16}} = \begin{bmatrix}
A_1^2A_2^2B^2 & 0 & A_1^0A_2^0B^0 & 0 & 0 & 0 & 0 & 0 \\
A_1^0A_2^0B^0 & 0 & A_1^2A_2^2B^2 & 0 & 0 & 0 & 0 & 0 \\
0 & A_1^2A_2^0B^0 & 0 & A_1^0A_2^2B^0 & 0 & 0 & 0 & 0 \\
0 & A_1^0A_2^2B^0 & 0 & A_1^2A_2^0B^0 & 0 & 0 & 0 & 0 \\
A_1^0A_2^0B^0 & 0 & A_1^2A_2^2B^2 & 0 & 0 & 0 & 0 & 0 \\
A_1^2A_2^2B^2 & 0 & A_1^0A_2^0B^0 & 0 & 0 & 0 & 0 & 0 \\
0 & A_1^0A_2^2B^0 & 0 & A_1^2A_2^0B^0 & 0 & 0 & 0 & 0 \\
0 & A_1^2A_2^0B^0 & 0 & A_1^0A_2^2B^0 & 0 & 0 & 0 & 0 \\
0 & 0 & 0 & 0 & A_1^2A_2^0B^0 & 0 & A_1^0A_2^2B^0 & 0 \\
0 & 0 & 0 & 0 & A_1^0A_2^2B^0 & 0 & A_1^2A_2^0B^0 & 0 \\
0 & 0 & 0 & 0 & 0 & A_1^2A_2^2B^{-2} & 0 & A_1^0A_2^0B^0 \\
0 & 0 & 0 & 0 & 0 & A_1^0A_2^0B^0 & 0 & A_1^2A_2^2B^{-2} \\
0 & 0 & 0 & 0 & A_1^0A_2^2B^0 & 0 & A_1^2A_2^0B^0 & 0 \\
0 & 0 & 0 & 0 & A_1^2A_2^0B^0 & 0 & A_1^0A_2^2B^0 & 0 \\
0 & 0 & 0 & 0 & 0 & A_1^0A_2^0B^0 & 0 & A_1^2A_2^2B^{-2} \\
0 & 0 & 0 & 0 & 0 & A_1^2A_2^2B^{-2} & 0 & A_1^0A_2^0B^0
\end{bmatrix} \quad (B.9)
$$

where $\mathbf{S}_{\mathbf{1\ to\ 8}}$ and $\mathbf{S}_{\mathbf{9\ to\ 16}}$ denote columns 1 to 8 and columns 9 to 16 of $\mathbf{S}$.

In each entry of the $\mathbf{S}$, the exponent of A_1 denotes the Euclidean distance between the correct and erroneous sequences transmitted across the first transmit antenna. Similarly, the exponent of A_2 denotes the Euclidean distance between the correct and erroneous sequence transmitted across the second transmitted antennas. The exponent of B denotes the value of the cross term for both transmit antennas. Thus, each entry in the matrix S takes the form $A_1^X A_2^Y B^Z$ and represents a one-step transition in the extended trellis from the state corresponding to the "row number," to the state corresponding to the "column number." If we were to compute the weight enumerating function directly from the extended trellis, the weight enumerating function will be the sum of the first entries in the first row of the matrix S^l where l denotes the length of each block in the block fading channel model and S^l denotes the l^{th} power of the matrix S.

For evaluating the bound for the system, we make use of the "Limiting Before Averaging" and Expurgation techniques in [33]. The idea of expurgating is to evaluate the bound by taking only the simple error events into account. Simple error events are those error events where once the erroneous codeword re-merges with the correct codeword on the extended trellis, it is assumed that the two codewords stay at the same state until the end. The expurgated state transition matrix is computed by introducing a new state, the 17th row of the extended matrix, to the extended state transition matrix, $\mathbf{S}$. This new state represents the paths that have previously diverged through the trellis are re-merging for the first time and no longer diverge. Thus, only simple error events are considered. Once the transition reaches this new state, it is assumed both paths are at one of the four states in Figure B.2 and do not diverge again. Thus, a new column needs to be added to the transition matrix to store the distances of the transitions that have previous led the transition to one of the $S_0^{(c)}S_0^{(e)}$, $S_1^{(c)}S_1^{(e)}$, $S_2^{(c)}S_2^{(e)}$, $S_3^{(c)}S_3^{(e)}$ states in Figure B.3. The 17 by 17 expurgated state transition matrix $\mathbf{S_{exp}}$ for the 4 state space time trellis code can be computed as

$$\mathbf{S_{exp1\ to\ 8}} = \begin{bmatrix}
A_1^0A_2^0B^0 & 0 & A_1^2A_2^2B^2 & 0 & 0 & 0 & 0 & 0 \\
0 & 0 & A_1^0A_2^0B^0 & 0 & 0 & 0 & 0 & 0 \\
0 & A_1^0A_2^2B^0 & 0 & A_1^2A_2^0B^0 & 0 & 0 & 0 & 0 \\
0 & A_1^2A_2^0B^0 & 0 & A_1^0A_2^2B^0 & 0 & 0 & 0 & 0 \\
0 & 0 & A_1^0A_2^0B^0 & 0 & 0 & 0 & 0 & 0 \\
A_1^0A_2^0B^0 & 0 & A_1^2A_2^2B^2 & 0 & 0 & 0 & 0 & 0 \\
0 & A_1^2A_2^0B^0 & 0 & A_1^0A_2^2B^0 & 0 & 0 & 0 & 0 \\
0 & A_1^0A_2^2B^0 & 0 & A_1^2A_2^0B^0 & 0 & 0 & 0 & 0 \\
0 & 0 & 0 & 0 & A_1^0A_2^2B^0 & 0 & A_1^2A_2^0B^0 & 0 \\
0 & 0 & 0 & 0 & A_1^2A_2^0B^0 & 0 & A_1^0A_2^2B^0 & 0 \\
0 & 0 & 0 & 0 & 0 & A_1^0A_2^0B^0 & 0 & A_1^2A_2^2B^{-2} \\
0 & 0 & 0 & 0 & 0 & 0 & 0 & A_1^0A_2^0B^0 \\
0 & 0 & 0 & 0 & A_1^2A_2^0B^0 & 0 & A_1^0A_2^2B^0 & 0 \\
0 & 0 & 0 & 0 & A_1^0A_2^2B^0 & 0 & A_1^2A_2^0B^0 & 0 \\
0 & 0 & 0 & 0 & 0 & 0 & 0 & A_1^0A_2^0B^0 \\
0 & 0 & 0 & 0 & 0 & A_1^0A_2^0B^0 & 0 & A_1^2A_2^2B^{-2} \\
0 & 0 & 0 & 0 & 0 & 0 & 0 & 0
\end{bmatrix}$$

$$\mathbf{S}_{\mathbf{exp}_{9\ \mathrm{to}\ 17}} = \begin{bmatrix}
A_1^2A_2^2B^2 & 0 & A_1^0A_2^0B^0 & 0 & 0 & 0 & 0 & 0 & 0 \\
A_1^0A_2^0B^0 & 0 & 0 & 0 & 0 & 0 & 0 & 0 & A_1^2A_2^2B^2 + A_1^2A_2^2B^2 \\
0 & A_1^2A_2^0B^0 & 0 & A_1^0A_2^2B^0 & 0 & 0 & 0 & 0 & 0 \\
0 & A_1^0A_2^2B^0 & 0 & A_1^2A_2^0B^0 & 0 & 0 & 0 & 0 & 0 \\
A_1^0A_2^0B^0 & 0 & 0 & 0 & 0 & 0 & 0 & 0 & A_1^2A_2^2B^2 + A_1^2A_2^2B^2 \\
A_1^2A_2^2B^2 & 0 & A_1^0A_2^0B^0 & 0 & 0 & 0 & 0 & 0 & 0 \\
0 & A_1^0A_2^2B^0 & 0 & A_1^2A_2^0B^0 & 0 & 0 & 0 & 0 & 0 \\
0 & A_1^2A_2^0B^0 & 0 & A_1^0A_2^2B^0 & 0 & 0 & 0 & 0 & 0 \\
0 & 0 & 0 & 0 & A_1^2A_2^0B^0 & 0 & A_1^0A_2^2B^0 & 0 & 0 \\
0 & 0 & 0 & 0 & A_1^0A_2^2B^0 & 0 & A_1^2A_2^0B^0 & 0 & 0 \\
0 & 0 & 0 & 0 & 0 & A_1^2A_2^2B^{-2} & 0 & A_1^0A_2^0B^0 & 0 \\
0 & 0 & 0 & 0 & 0 & A_1^0A_2^0B^0 & 0 & 0 & A_1^2A_2^2B^{-2} + A_1^2A_2^2B^{-2} \\
0 & 0 & 0 & 0 & A_1^0A_2^2B^0 & 0 & A_1^2A_2^0B^0 & 0 & 0 \\
0 & 0 & 0 & 0 & A_1^2A_2^0B^0 & 0 & A_1^0A_2^2B^0 & 0 & 0 \\
0 & 0 & 0 & 0 & 0 & A_1^0A_2^0B^0 & 0 & 0 & A_1^2A_2^2B^{-2} + A_1^2A_2^2B^{-2} \\
0 & 0 & 0 & 0 & 0 & A_1^2A_2^2B^{-2} & 0 & A_1^0A_2^0B^0 & 0 \\
0 & 0 & 0 & 0 & 0 & 0 & 0 & 0 & 2
\end{bmatrix} \quad \text{(B.10)}$$

where $\mathbf{S}_{\mathbf{exp}_{1\ \mathrm{to}\ 8}}$ and $\mathbf{S}_{\mathbf{exp}_{9\ \mathrm{to}\ 17}}$ denote columns 1 to 8 and columns 9 to 17 of $\mathbf{S}_{\mathbf{exp}}$. The corresponding extended trellis with expurgation is shown in Figure B.4.

Since the convolutional codes used in this thesis is terminated, we need to multiply the expurgated transition matrix by a termination vector to ensure the frame ends in the zero state. The termination vector can be easily computed as

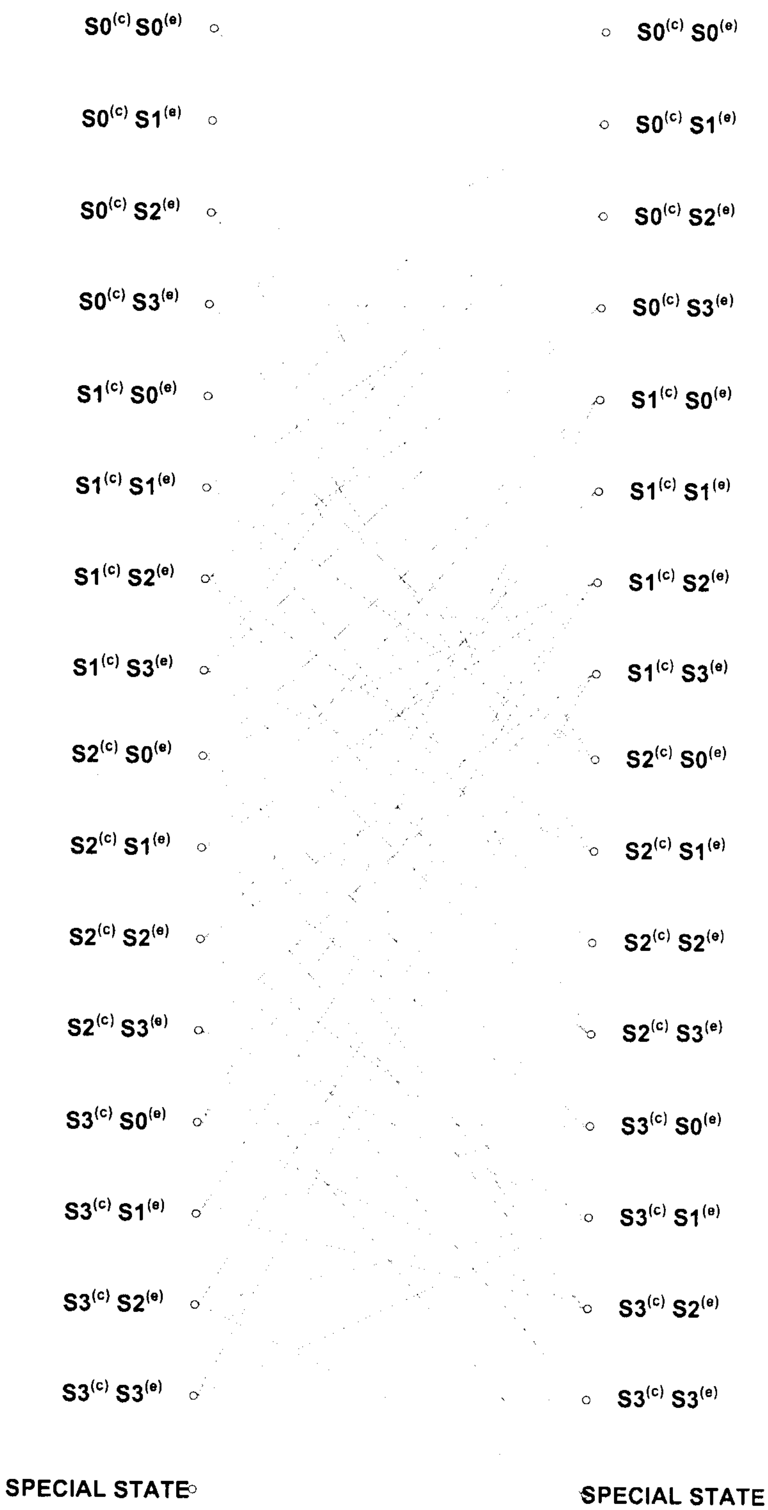

Figure B.4: Extended Trellis after Expurgation for the 4 State Space Time Trellis Code.

$$
\mathbf{S_{term}} = \begin{bmatrix} 1 \\ A_1^2A_2^2B^2 \\ A_1^2A_2^4B^2 \\ A_1^4A_2^2B^2 \\ A_1^2A_2^2B^2 \\ 1 \\ A_1^4A_2^2B^2 \\ A_1^2A_2^4B^2 \\ A_1^2A_2^4B^2 \\ A_1^4A_2^2B^2 \\ 1 \\ A_1^2A_2^2B^{-2} \\ A_1^4A_2^2B^2 \\ A_1^2A_2^4B^2 \\ A_1^2A_2^2B^{-2} \\ 1 \\ 1 \end{bmatrix} \tag{B.11}
$$

Similar to the non-expurgated case, the weight enumerating function for the space time trellis code is obtained from the sum of the first entry in the vector $\mathbf{S^l_{exp}S_{term}}$.

If different codes are used to encode the information bits for the two blocks (i.e. $K = 4$ convolutional code with $g = [15\ 17]$ for user 1 and $g = [13\ 15]$ for user 2), then a different weight enumerating function has to be derived for each block. The example shown in this Appendix is for the case where the users use the same code to encode the information bits in each block. The derivation is similar to that as in [33], but a different code is used.

Appendix C

SNR Definition

Recall from Chapter 2 that the received signal at time t of segment k from user 1 is

$$r_t = \sum_{i=1}^{2} \sqrt{E_s} g_{1,i} c_{t,i}^k + n_t. \tag{C.1}$$

From this, the average signal power is

$$\begin{aligned} & E_s E\{|G_{1,1}|^2\} E\{|c_{t,1}^k|^2\} + E_s E\{|G_{1,2}|^2\} E\{|c_{t,2}^k|^2\} \\ & + 2E_s E\{G_{1,1} G_{1,2}^*\} E\{c_{t,1}^k c_{t,2}^k\} \\ & = 2E_s \sigma_G^2 \end{aligned} \tag{C.2}$$

and the noise power is N_0

Hence, the signal to noise ratio is

$$SNR = \frac{2E_s \sigma_G^2}{N_0} \tag{C.3}$$

Assuming $E_b = 1$, then $E_s = RE_b = \frac{1}{2}$ since the overall rate, R, of the system is $\frac{1}{2}$

Bibliography

[1] J. G. Proakis, "*Digital Communications*", McGraw Hill, 4th edition, 2001.

[2] T. S. Rappaport, "*Wireless Communications Principles and Practice*", Prentice Hall 2002.

[3] A. Paulraj, R. Nabar and D. Gore, "*Introduction to Space-Time Wireless Communications*", Cambridge University Press 2003.

[4] V. Tarokh, N. Seshadri, and A. R. Calderbank, "Space-Time Codes for High Data Rate Wireless Communication: Performance Criterion and Code Contruction", *IEEE Transactions on Information Theory*, vol. 44, no. 2, pp 744-765, March 1998.

[5] S. M. Alamouti, "A Simple Transmit Diversity Technique for Wireless Communications", *IEEE Journal on Selected Areas in Communications*, vol. 16, no. 8, pp. 1451-1458, October 1998.

[6] A. Sendonaris, E. Erkip, and B. Aazhang, "User cooperation diversity - Part I: System Description", *IEEE Trans. Commun.*, vol. 51, pp. 1927-1938, November 2003.

[7] A. Sendonaris, E. Erkip, and B. Aazhang, "User cooperation diversity - Part II: Implementation aspects and performance analysis", *IEEE Trans. Commun.*, vol. 51, pp. 1939-1948, November 2003.

[8] J. N. Laneman, D. N. C. Tse, and G. W. Wornell, "Cooperative diversity in wireless networks: Efficient protocols and outage behavior", *IEEE Transactions on Information Theory*, vol. 50, no. 12, pp. 3062-3080, December 2004.

[9] J. N. Laneman "Cooperative diversity in wireless networks: Algorithms and architectures," Ph. D. dissertation, Massachusetts Institute of Technology, August 2002.

[10] D. Gu, "Performance Analysis of a Transmit Diversity Scheme in Correlated Fading with Imperfect Channel Estimation," *MASc. Thesis*, Department of Electrical and Computer Engineering, UBC, March 2003.

[11] T. Zheng, "Performance Degradation of a Transmit Diversity Scheme Due to Correlated Fading," *MASc. Thesis*, Department of Electrical and Computer Engineering, UBC, February 2005.

[12] Giorgio Taricco, "Space-Time Decoding With Imperfect Channel Estimation", *IEEE Transactions on Communications*, vol. 4, no. 4, pp. 1874-1888, July 2005.

[13] A. Hedayat, "Analysis of Space-Time Coding in Correlated Channels", *IEEE Transactions on Communications*, vol. 4, no. 6, pp. 2882-2891, November 2005.

[14] A. Stefanov and E. Erkip, "Cooperative Space Time Coding for Wireless networks", *IEEE Transactions on Communications*, vol. 53, no.11, pp. 1804-1809, November 2005.

[15] T. M. Cover and A. El Gamal, "Capacity Theorems for the Relay Channel", *IEEE Transactions on Information Theory*, vol. 25, no. 5, pp. 572-584, September 1979.

[16] T. Hunter and A. Nosratinia, "Cooperative diversity through coding", *Proc. IEEE Int. Symp. Inf. Theory*, Lausanne, Switzerland, pp. 220-220, June 2002.

[17] R. Knopp and P. A. Humblet, "On Coding for Block Fading Channels", *IEEE Transaction on Information Theory*, vol. 46, no. 1, pp. 189-205, Janurary 2000.

[18] S. A. Kassam, *Signal Detection in non-Gaussian Noise*. Springer-Verlag, 1987.

[19] S. Miyamoto, M. Katayama, and N. Morinaga, "Performance Analysis of QAM Systems Under Class A Impulsive Noise Environment", *IEEE Transactions on Electromagnetic Compatibility*, vol. 37, no. 2, May 1995.

[20] J. Haring, and A. J. H. Vinck, "Performance Bounds for Optimum and Suboptimum Reception Under Class-A Impulsive Noise", *IEEE Transactions on Communications*, vol. 50, no. 7, July 2002.

[21] J. N. Laneman, and G. W. Wornell, "Energy-efficient antenna sharing and relaying for wireless networks", *IEEE Wireless Communications and Networking Conference (WCNC)*, vol. 1, pp. 7-12, September 2000.

[22] T. E. Hunter and A. Nosratinia, "Coded Cooperation under slow fading, fast fading, and power control", in *Proc. Allerton Conference on Communications, Control, and Computing*, Pacific Grove, CA, November 2002.

[23] M. Janani, A. Hedayat, T. E. Hunter, and A. Nosratinia, "Coded Cooperation in Wireless Communications: Space-Time Transmission and Iterative Decoding", *IEEE Transactions on Signal Processing*, vol. 52, no. 2, pp. 362-371, February 2004.

[24] A. Stefanov and E. Erkip, "Cooperative Coding for Wireless networks", *IEEE Transactions on Communications*, vol. 52, no.9, pp. 1470-1476, September 2004.

[25] H. El Gamal and A. R. Hammons, Jr., "On the design of algebraic space-time codes for MIMO block-fading channels", *IEEE Transactions on Information Theory*, vol. 49, no. 1, pp. 151-163, Janurary 2003.

[26] A. R. Hammons, Jr. and H. El Gamal, "On the theory of space-time codes for PSK modulation", *IEEE Transactions on Information Theory*, vol. 46, no. 3, pp. 524-542, March 2000.

[27] W. C. Y. Lee, *Mobile Communications Design Fundamentals*, 2^{nd} edition, Wiley, 1993.

[28] D. Lin, "Performance Analysis of Viterbi Decoding in Rayleigh Fading with Channel Estimation Error", *MASc. Thesis*, Department of Electrical and Computer Engineering, UBC, March 2006.

[29] V. Tarokh, H. Jafarkhani, and A. R. Calderbank, "Space-Time Block Coding for Wireless Communications: Performance Results", *IEEE Journal on Selected Areas in Communications*, vol. 17, no. 3, pp 451-460, March 1999.

[30] V. Tarokh, A. Naguib, N. Seshadri, and A. R. Calderbank, "Errata to Space-Time Codes for High Data Rate Wireless Communication: Performance Criteria in the Presence of Channel Estimation Errors, Mobility, and Multiple Paths", *IEEE Transactions on Communications*, vol. 51, no. 12, pp 2141, December 2003.

[31] V. Tarokh, A. Naguib, N. Seshadri, and A. R. Calderbank, "Space-Time Codes for High Data Rate Wireless Communication: Performance Criteria in the Presence of Channel Estimation Errors, Mobility, and Multiple Paths", *IEEE Transactions on Communications*, vol. 47, no. 2, pp 199-207, Februrary 1999.

[32] E. Malkamaki and H. Leib "Evaluating the Performance of Convolutional Codes over Block Fading Channels", *IEEE Transactions on Information Theory*, vol. 45, pp. 1643-1646, July 1999.

[33] A. Stefanov and T. M. Duman, "Performance Bounds for Space Time Trellis Codes", *IEEE Transactions on Information Theory*, vol. 49, no.9, pp. 2134-2140, September 2003.

[34] A. Stefanov and E. Erkip, "On the Performance Analysis of Cooperative Space Time Coded Systems", *IEEE Wireless Communications and Networking Conference (WCNC)*, vol. 2, pp. 729 - 734, March 2003.

[35] Z. Lin, E. Erkip, and A. Stefanov "Cooperative regions and partner choice in coded Cooperative systems", *IEEE Transactions on Communications*, vol. 54, Issue 7, pp. 1323 - 1334, July 2006.

[36] D. Aktas and M.P.Fitz, "Computing the distance spectrum of space-time trellis codes", *IEEE Wireless Communications and Networking Conference (WCNC)*, vol. 1, pp. 51 - 55, September 2000.